Journal of Sound and Vibration 437 (2018) 389–409

Contents lists available at ScienceDirect

Journal of Sound and Vibration

journal homepage: www.elsevier.com/locate/jsvi

On the extension of cylindrical acoustic waves to acoustic-vortical-entropy waves in a flow with rigid body swirl

L.M.B.C. Campos, A.C. Marta *

Center for Aeronautical and Space Science and Technology, IDMEC, Instituto Superior Técnico, Universidade de Lisboa, Av. Rovisco Pais 1, 1049-001 Lisboa, Portugal

ARTICLE INFO

Article history:
Received 29 November 2017
Revised 9 July 2018
Accepted 6 September 2018
Available online 11 September 2018
Handling Editor: Y. Auregan

Keywords:
Aeroacoustics
Acoustic-vortical-entropy waves
Swirling flow instabilities
Non-isentropic perturbations

ABSTRACT

The noise of jet and rocket engines involves the coupling of sound to swirling flows and to heat exchanges leading in the more complex cases of triple interactions to acoustic-vortical-entropy (AVE) waves. The present paper presents the derivation of the AVE equation for axisymmetric linear non-dissipative, compressible perturbations of a non-homentropic, swirling mean flow, with constant axial velocity and constant angular velocity for a perfect gas with constant density. The axisymmetric AVE wave equation is obtained for the radial velocity perturbation, specifying its radial dependence for any frequency and axial wavenumber. The AVE wave equation in the case of zero axial wavenumber, corresponding to cylindrical AVE waves, has no singularities for finite radius, including the sonic radius, where the isothermal Mach number for the swirl velocity is unity. The exact solution of the AVE wave equation for the fundamental axisymmetric mode with zero axial wavenumber is obtained without any restriction on frequency, as series expansions of Gaussian hypergeometric type: (i) covering the whole flow region; (ii) specifying the wave field at the sonic radius; (iii) specifying near-axis and asymptotic scaling for small and large radius. Using polarization relations among wave variables specifies exactly and allows the plotting of the perturbations of: (i,ii) the radial and azimuthal velocity; (iii,iv) pressure and mass density; (v,vi) entropy and temperature. Thus the extension of cylindrical acoustic waves, that are specified by Bessel functions, to cylindrical acoustic-vortical-entropy waves, is specified by Gaussian hypergeometric functions.

1. Introduction

The noise of aircraft engines is a major limitation on airport operations, and the subject of ever more stringent certification rules, aiming to limit the total noise exposure as air traffic grows. The noise of the rocket engines of space launchers is sufficiently high to cause structural damage and require payloads like satellites to be tested for acoustic fatigue in reverberant chambers. The literature on aircraft and rocket engine noise usually considers purely acoustic waves, although coupling with other modes occur in: (i) inlet ducts due to the shear flow in the wall boundary layers; (ii) in turbine exhausts due to the downstream swirling flow; (iii) in the combustion chambers and other heat generation and exchange processes involving non-isentropic flows. The simplest mean flow for which there are interacting acoustic, vortical and entropy perturbations is an axisymmetric non-homentropic flow with uniform axial velocity and rigid body swirl; this sample problem is of interest in itself relating to

* Corresponding author.
E-mail addresses: luis.campos@tecnico.ulisboa.pt (L.M.B.C. Campos), andre.marta@tecnico.ulisboa.pt (A.C. Marta).

https://doi.org/10.1016/j.jsv.2018.09.017

waves in nozzles with swirl and heat exchange.

There are [1–3] three types of waves in a fluid in the absence of external restoring forces [4,5], namely: (i) sound waves that are longitudinal and compressive; (ii) vortical waves that are transversal, hence incompressible; (iii) entropy modes associated with heat exchanges, hence non-homentropic flow. The acoustic modes receive most attention because for an homogeneous uniform mean flow: firstly, the acoustic modes satisfy the convected wave equation for uniform motion and the classical wave equation in a medium at rest [6–13]; secondly, by the Kelvin circulation theorem the circulation along a loop convected with the mean flow is constant [14–18]; thirdly, in homentropic conditions there are no entropy modes. The most general conditions for the existence of purely acoustic modes, decoupled from vortical-entropy modes, is a potential homentropic mean flow, that may be compressible, and leads to the high-speed wave equation [19–21] that reduces to the convected wave equation [22–24] in two cases: (i) uniform flow; (ii) low Mach number steady non-uniform flow. The presence of vorticity leads to acoustic-vortical waves [25–30], in a compressible sheared [31–44] or swirling [45–57] mean flow. The present paper considers a further extension to acoustic-vortical-entropy waves [57] that specify the stability of a compressible, vortical and non-homentropic mean flow.

The acoustic, vortical and entropy modes [1–3] are decoupled in a medium at rest and become coupled in sheared and/or swirling non-homentropic mean flows. The first derivation of the acoustic-vortical (AV) wave equation [46] used a decomposition of the velocity perturbation into an irrotational and a vortical part. The AV waves were considered for specific swirl profiles [47–49] such as rigid body and potential vortex. These two profiles were also considered as particular cases of AV waves in an axisymmetric mean flow with shear and swirl arbitrary functions of the radius, assuming constant density [49]; the latter condition can be replaced by that of an homentropic mean flow [30]. Besides the propagation [30,45–52], also the generation [53–56] of AV waves has been considered. The more general case of AVE waves has been considered [57] as isentropic non-axisymmetric longitudinally propagating perturbations of a non-homentropic mean flow with shear and swirl arbitrary functions of the radius in the WKB approximation of high-frequency, which excludes critical layers. The present paper derives the AVE wave equation also for isentropic perturbations of a non-homentropic mean flow, restricting to a uniform axial flow and rigid body swirl and axisymmetric modes, without restriction of frequency, showing that a critical layer exists for isothermal sound speed equal to the phase speed based on the Doppler shifted frequency. The critical layer does not exist for zero axial wavenumber, that is for cylindrical AVE waves, in which case the exact solution valid for all frequencies and distances is obtained in terms of Gaussian hypergeometric functions.

The linearized Euler equations (LEE) contain all these modes, but consist of one vector (momentum) and three scalar (continuity, energy and state) equations with six variables (velocity vector, pressure, density and entropy). In this formulation, the 'wave operator' is a 6×6 matrix that cannot be readily compared to a scalar wave equation for one variable like the pressure perturbation. This paper presents a scalar wave equation for a single wave variable (the radial velocity) that generalizes the classic wave equation for sound and the acoustic-vortical wave equation in a swirling flow. This derivation involves elimination among the 6 LEE equations for one variable only, namely the radial velocity, that determines through polarization relations all other variables, namely the perturbations of the density, pressure, temperature, entropy and axial and azimuthal components of the velocity. There is substantial evidence in the literature of the presence of non-acoustic perturbations in nozzle flows, and the derivation of an acoustic-vortical-entropy (AVE) equation aims to address this limitation of current wave equations, by allowing the interaction of all three effects.

The radial dependence of the fundamental axisymmetric mode of non-dissipative AVE waves, in a uniform mean flow with rigid body swirl of a perfect gas with constant density is specified exactly, without any restriction on frequency, by a linear second-order differential equation with four regular singularities, of which one is a critical layer. The critical layer does not exist for zero axial wavenumber, corresponding to cylindrical AVE waves that depend only on time and radial distance. The radial dependence of the cylindrical AVE equation is thus specified by a linear second-order differential equation with three regular singularities, whose solution is (Section 3) specified by Gaussian hypergeometric functions [58–60]. These replace the Bessel functions [61–63] that specify acoustic cylindrical waves in an homentropic medium at rest or in uniform motion but without swirl. The three singularities of the cylindrical AVE wav equation are firstly the origin specifying the inner wave field, secondly the point at infinity specifying the asymptotic wave field, and thirdly the sonic point where the swirl velocity equals the isothermal sound speed. The latter is an apparent singularity of the differential equation [64–66] since the wave field is finite at the sonic condition. The solution around the sonic condition matches continuously the inner and asymptotic wave fields.

Since both the cylindrical AVE wave equation and its solutions are exact, they specify the wave field for all frequencies and radial distances. The cylindrical AVE wave equation is an exact linearization of the equations of motion, and thus its solutions specify the stability of the non-homentropic, non-dissipative uniform flow with rigid body swirl of a perfect gas with constant density. Since the dependence on time is sinusoidal with fixed frequency, the stability for cylindrical perturbations can only be considered in the radial direction. It is shown (Fig. 1) that as the radial distance tends to infinity the perturbations are waves with finite amplitude if the frequency exceeds the angular velocity (with a factor of order unity); conversely, if the frequency is less than the angular velocity, the perturbations grow radially and are unbounded. These conclusions broadly agree with earlier results [67–69] on the stability of vortical flows. The distinction between cylindrical AVE waves with finite radial amplitude and radially unbounded perturbations of the mean flow is illustrated by plotting the radial dependence of the first six modes in a rigid cylindrical duct (Section 4) for the perturbations of the radial and azimuthal velocities, pressure, density, temperature and entropy (Figs. 2–7).

2. The acoustic-vortical-entropy wave equation

The acoustic-vortical-entropy waves are considered as small axisymmetric perturbations of a non-dissipative, non-homentropic mean flow (Subsection 2.1) with uniform axial velocity and rigid body swirl (Subsection 2.2) of a perfect gas with constant mass density. Elimination for the radial velocity perturbation leads to the acoustic-vortical-entropy wave equation, its solutions specify through polarization relations also the perturbations of azimuthal velocity, pressure, mass density, temperature and entropy (Subsection 2.3).

2.1. Compressible, vortical, isentropic, non-homentropic flow of a perfect gas

The fundamental equations of fluid mechanics are written in cylindrical coordinates (r, φ, z) in axisymmetric form without φ-dependence $(\partial/\partial\varphi = 0)$:

(i) mass conservation:

$$\mathrm{D}\Gamma/\mathrm{d}t = -\Gamma\boldsymbol{\nabla}\cdot\boldsymbol{V} = -\frac{\Gamma}{r}\frac{\partial}{\partial r}\left(rV_r\right) - \Gamma\frac{\partial V_z}{\partial z}\,; \tag{1}$$

(ii) inviscid momentum:

$$\Gamma\left(\mathrm{D}V_r/\mathrm{d}t - r^{-1}V_\varphi^2\right) + \partial_r P = 0, \tag{2a}$$

$$\Gamma\left(\mathrm{D}V_\varphi/\mathrm{d}t + r^{-1}V_r V_\varphi\right) = 0, \tag{2b}$$

$$\Gamma \mathrm{D}V_z/\mathrm{d}t + \partial_z P = 0; \tag{2c}$$

(iii) energy neglecting dissipative effects, namely heat conduction and viscosity:

$$\mathrm{D}S/\mathrm{d}t = 0\,; \tag{3}$$

(iv) state:

$$\mathrm{D}P/\mathrm{d}t = c^2\mathrm{D}\Gamma/\mathrm{d}t + \beta\mathrm{D}S/\mathrm{d}t\,; \tag{4}$$

where Γ is the mass density, P the pressure, $\boldsymbol{V}$ the velocity, T the temperature, S the entropy, the material derivative is denoted by

$$\mathrm{D}/\mathrm{d}t = \partial/\partial t + \boldsymbol{V}\cdot\boldsymbol{\nabla} = \partial/\partial t + V_r\partial_r + V_z\partial_z \tag{5a,b}$$

and the equation of state in the form (6a) specifies the coefficients in (4),

$$P = P(\Gamma, S)\,:\, c^2 \equiv \left(\frac{\partial P}{\partial \Gamma}\right)_S, \quad \beta = \left(\frac{\partial P}{\partial S}\right)_\Gamma, \tag{6a-c}$$

namely the adiabatic sound speed (6b) and the non-isentropic coefficient (6c). Chemical reactions are not considered explicitly and appear through the entropy coefficient. The adiabatic sound speed (6b) is sufficient for acoustic-vortical (AV) waves and the non-isentropic coefficient (6c) may be necessary for acoustic-vortical-entropy (AVE) waves.

In the sequel is considered the case of a perfect gas, with the equations of state (7a) and entropy (7b),

$$P = R\Gamma T, \quad S = C_V \log P - C_P \log \Gamma + \mathrm{const}, \tag{7a,b}$$

involving the gas constant R and specific heats at constant volume C_V and pressure C_P that are related by (8a,c,d) involving the adiabatic exponent (8b),

$$R = C_P - C_V, \quad \gamma = \frac{C_P}{C_V}\,:\, C_V = \frac{R}{\gamma-1}, \quad C_P = \frac{\gamma R}{\gamma - 1}\,. \tag{8a-d}$$

From the entropy equation (7b) it follows

$$\mathrm{d}S = C_V\frac{\mathrm{d}P}{P} - C_P\frac{\mathrm{d}\Gamma}{\Gamma}\,; \tag{9a}$$

in the adiabatic case (9b) the sound speed is given by (9c),

$$\mathrm{d}S = 0\,:\, c^2 = \left(\frac{\partial P}{\partial \Gamma}\right)_S = \frac{C_P}{C_V}\frac{P}{\Gamma} = \gamma\frac{P}{\Gamma} = \gamma RT\,. \tag{9b,c}$$

The non-isentropic coefficient (6c) may be calculated (10b) from the specific heat at constant volume (10a),

$$C_V = T\left(\frac{\partial S}{\partial T}\right)_\Gamma\,:\, \beta = \left(\frac{\partial P}{\partial T}\right)_\Gamma \Big/ \left(\frac{\partial S}{\partial T}\right)_\Gamma = \frac{T}{C_V}\left(\frac{\partial P}{\partial T}\right)_\Gamma\,; \tag{10a,b}$$

in the case of a perfect gas (7a) follows (11a,b),

$$\beta = \frac{T}{C_V} R\Gamma = \frac{P}{C_V} = \frac{\gamma - 1}{R} P, \tag{11a-c}$$

and also (11c) using (8c).

2.2. Linear perturbation of a uniform flow with rigid body swirl

The mean flow (subscript zero) is assumed to consist (12a) of a uniform axial velocity plus a rigid body swirl,

$$\boldsymbol{V}_0 = \boldsymbol{e}_z U + \boldsymbol{e}_\varphi \Omega r, \quad \boldsymbol{\varpi} = \nabla \times \boldsymbol{V}_0 = \boldsymbol{e}_z 2\Omega, \tag{12a,b}$$

so that the vorticity (12b) is twice the angular velocity. The linearized material derivative (5a) for the axial mean flow (12a) is (13a),

$$\delta/\mathrm{d}t \equiv \partial/\partial t + U\partial/\partial z, \quad \nabla \cdot \boldsymbol{V}_0 = 0, \tag{13a,b}$$

and the mean flow velocity (12a) has zero divergence (13b). Applying the fundamental equations to the mean flow (12a) it follows that: (i-ii) the mass density (1) and entropy (3) can depend only on the radius (14a,b); (iii) there is a radial pressure gradient (2a) due to the centrifugal force (14c),

$$\rho_0 = \rho_0(r) \quad s_0 = s_0(r) : p_0' \equiv \mathrm{d}p_0/\mathrm{d}r = \rho_0 \Omega^2 r \,. \tag{14a-c}$$

The mean flow has a solenoidal (13b) velocity (12a), and thus causes no compression, even in an compressible fluid. The distinction should be made between incompressible flow and incompressible fluid. The fluid is compressible, the mean flow (12a) causes no compression (13b), and thus the compressions are entirely due to the wave perturbations, for which the adiabatic or isothermal sound speeds could be relevant. A similar situation applies to an unidirectional shear flow that causes no compression to a compressible fluid, so that compressions are solely due to acoustic-vortical wave perturbations of shear type [25–44]. A particular case of (14a) is a constant mean flow mass density (15a) that leads to the pressure (15c) where (15b) is the pressure on axis,

$$\rho_0 = \text{const}, \quad p_{00} = p_0(0) : p_0(r) = p_{00} + \frac{1}{2}\rho_0 \Omega^2 r^2 \,. \tag{15a-c}$$

The adiabatic sound speed (9c) and non-isentropic coefficient (11b) are given in the mean flow respectively by (16b) and (16c), where (16a) is the adiabatic sound speed on the axis,

$$c_{00}^2 = \gamma \frac{p_{00}}{\rho_0} : \left[c_0(r)\right]^2 = \gamma \frac{p_0(r)}{\rho_0} = c_{00}^2 + \frac{\gamma}{2}\Omega^2 r^2, \quad \beta_0(r) = \frac{p_0(r)}{C_V} \,. \tag{16a-c}$$

The adiabatic sound speed (16b) can also be written in the form (17a) where (17b) is the reference radius,

$$[c_0(r)]^2 = c_{00}^2 [1 + (r/r_0)^2], \quad r_0 = (c_{00}/\Omega)\sqrt{2/\gamma} \,. \tag{17a,b}$$

The entropy in the mean flow (18a),

$$s_0 = C_V \log p_0 - C_P \log \rho_0 + \text{const}, \tag{18a}$$

has radial gradient (18b),

$$s_0' = C_V \frac{p_0'}{p_0} = \frac{p_0'}{\beta_0} = \frac{\rho_0 \Omega^2 r}{\beta_0} = C_V \frac{\rho_0 \Omega^2 r}{p_0} = C_V \gamma \frac{\Omega^2 r}{c_0^2} = C_P \frac{\Omega^2 r}{c_0^2} \,. \tag{18b}$$

Thus the uniform axial flow with rigid body swirl (12a) and a constant mass density (15a) implies the radial dependences of the pressure (15b,c), adiabatic sound speed (17a,b) and also the existence of an entropy gradient (18b). The linear perturbation of this mean flow is considered next.

The total flow is assumed to consist of the mean flow plus a perturbation depending on time t, radial r and axial z coordinate, but not on the azimuthal coordinate φ, thus excluding circumferential modes,

$$V_r(r,z,t) = v_r(r,z,t), \quad V_\varphi(r,z,t) = \Omega r + v_\varphi(r,z,t), \quad V_z(r,z,t) = U + v_z(r,z,t), \tag{19a-c}$$

$$P(r,z,t) = p_0(r) + p(r,z,t), \quad \Gamma(r,z,t) = \rho_0 + \rho(r,z,t), \quad S(r,z,t) = s_0(r) + s(r,z,t) \,. \tag{19d-f}$$

Since the mean flow properties, that appear as coefficients in the linearization, depend on r but not (z,t), the Fourier transform is made (20) with frequency ω and axial wavenumber k,

$$f(r,z,t) = \int_{-\infty}^{+\infty} \mathrm{d}k \int_{-\infty}^{+\infty} \mathrm{d}\omega, e^{\mathrm{i}(kx - \omega t)} \tilde{f}(r,k,\omega)\,; \tag{20}$$

for example the linearized material derivative for the axial flow (13a) leads (21a) to the frequency (21b) Doppler shifted by the axial mean flow,

$$\delta/\mathrm{d}t \to -\mathrm{i}\omega_* : \omega_* = \omega - kU. \tag{21a,b}$$

Substituting (19a–f) in (1,2a–c,3,4) and linearizing leads to

$$\mathrm{i}\omega_* r\tilde{\rho} - \rho_0 (r\tilde{v}_r)' - \mathrm{i}\rho_0 kr\tilde{v}_z = 0, \tag{22a}$$

$$\mathrm{i}\rho_0\omega_*\tilde{v}_r + 2\Omega\rho_0\tilde{v}_\varphi + \Omega^2 r\tilde{\rho} - \tilde{p}' = 0, \tag{22b}$$

$$\mathrm{i}\omega_*\tilde{v}_\varphi - 2\Omega\tilde{v}_r = 0, \tag{22c}$$

$$\rho_0\omega_*\tilde{v}_z - k\tilde{p} = 0, \tag{22d}$$

$$\mathrm{i}\omega_*\tilde{s} = s_0'\tilde{v}_r = C_P\frac{\Omega^2}{c_0^2}r\tilde{v}_r, \tag{22e}$$

$$\tilde{p} = c_0^2\tilde{\rho} + \beta_0\tilde{s}, \tag{22f}$$

where prime denotes derivative with regard to the radius. The last equation (22f) follows from linearization of (6a) using (6b,c). The equation of energy (3) implies that the mean flow is isentropic (23a), that is consistent with the entropy being a function of the radius (14b),

$$\frac{\delta s_0}{\mathrm{d}t} = 0 : 0 = \frac{\mathrm{D}(s+s_0)}{\mathrm{d}t} - \frac{\delta s_0}{\mathrm{d}t}, \tag{23a,b}$$

subtracting the mean state (23a) from the exact (3) energy equation leads to (23b), that is linearized (24a),

$$0 = \frac{\mathrm{D}s}{\mathrm{d}t} + \frac{\mathrm{D}s_0}{\mathrm{d}t} - \frac{\delta s_0}{\mathrm{d}t} = \frac{\delta s}{\mathrm{d}t} - \boldsymbol{V}\cdot\boldsymbol{\nabla}s_0; \tag{24a}$$

from (24a) follows (24b),

$$\frac{\delta s}{\mathrm{d}t} = -\left(\boldsymbol{V}\cdot\boldsymbol{\nabla}s_0\right), \quad \mathrm{i}\omega_*\tilde{s} = s_0'\tilde{v}_r, \tag{24b,c}$$

proving (24c)≡(22e).

2.3. Wave equation for the radial velocity and polarization relations

Of the six variables in (22a–f) four $(\tilde{v}_r, \tilde{v}_\varphi, \tilde{\rho}, \tilde{s})$ are expressible (22d,c,e,a) in terms of $(\tilde{p}, \tilde{v}_r)$,

$$\tilde{v}_z = \frac{k}{\rho_0\omega_*}\tilde{p}, \quad \tilde{v}_\varphi = -\mathrm{i}\frac{2\Omega}{\omega_*}\tilde{v}_r, \quad \tilde{s} = -\mathrm{i}C_P\frac{\Omega^2}{c_0^2\omega_*}r\tilde{v}_r. \tag{25a-c}$$

$$\tilde{\rho} = -\mathrm{i}\frac{\rho_0}{\omega_* r}(r\tilde{v}_r)' + \frac{k^2}{\omega_*^2}\tilde{p}. \tag{25d}$$

Substituting (25c,d) in (22f) leads to

$$\mathrm{i}\tilde{p}\left(\omega_* - k^2c_0^2/\omega_*\right) = \rho_0\left(\Omega^2 r + c_0^2/r\right)\tilde{v}_r + \rho_0 c_0^2\tilde{v}_r', \tag{26}$$

the pressure in terms of the radial velocity spectrum.

Substituting (25b,d) in (22b) leads to a relation between $\tilde{p}$ and $\tilde{v}_r$ distinct from (26), namely

$$\mathrm{i}\rho_0\left[\left(\omega_*^2 - 5\Omega^2\right)\tilde{v}_r - \Omega^2 r\tilde{v}_r'\right] = \omega_*\tilde{p}' - \frac{k^2\Omega^2 r}{\omega_*}\tilde{p}. \tag{27}$$

Substituting $\tilde{p}$ from (26) in (27) leads to the acoustic-vortical-entropy wave equation for the radial velocity perturbation spectrum,

$$c_0^2\tilde{v}_r'' + A\tilde{v}_r' + B\tilde{v}_r = 0, \tag{28}$$

with coefficients

$$X \equiv 1 - k^2c_0^2/\omega_*^2 : A = c_0^2/r + X\left[c_0^2/X\right]', \tag{29a,b}$$

$$B = \left(\omega_*^2 - 5\Omega^2\right) X - k^2\Omega^2 \left(\Omega^2 r^2 + c_0^2\right) / \omega_*^2 + X\left[\left(\Omega^2 r + c_0^2/r\right)/X\right]' . \tag{29c}$$

In conclusion the linear, non-dissipative axisymmetric compressive, vortical, non-adiabatic perturbations of a non-homentropic uniform axial flow with rigid body swirl (12a) of a perfect gas with constant mass density, with frequency ω and axial wavenumber k, lead (20) to the acoustic-vortical-entropy wave equation (28) with coefficients (29a–c) satisfied by the radial velocity perturbation spectrum.

The other wave variables are specified by the following polarization relations: (i–iii) the pressure (26), entropy (25c) and azimuthal velocity (25b) perturbation spectra; (iv–v) the axial velocity (25a) and mass density (25d) perturbation spectra lead, by (26), respectively to (30a) and (30b),

$$\widetilde{v}_z = -\mathrm{i}k\left[\left(\Omega^2 r + c_0^2/r\right)\widetilde{v}_r + c_0^2\widetilde{v}_r'\right] / \left(\omega_*^2 - k^2c_0^2\right), \tag{30a}$$

$$\mathrm{i}\widetilde{\rho}/\rho_0 = \widetilde{v}_r'/\omega_* + \widetilde{v}_r/(\omega_* r) + k^2\left[\left(\Omega r + c_0^2/r\right)\widetilde{v}_r + c_0^2\widetilde{v}_r'\right] / \left(\omega_*^3 - k^2c_0^2\omega_*\right). \tag{30b}$$

The temperature perturbation spectrum follows from the equation of state (7a),

$$R\widetilde{T} = \frac{\widetilde{p}}{\rho_0} - \frac{p_0}{\rho_0^2}\widetilde{\rho} = \frac{\mathrm{i}c_0^2}{\omega_*\gamma}\left(\widetilde{v}_r' + \widetilde{v}_r/r\right) - \mathrm{i}\frac{\omega_* - k^2c_0^2/\gamma\omega_*}{\omega_*^2 - k^2c_0^2}\left[\left(\Omega^2 r + c_0^2/r\right)\widetilde{v}_r + c_0^2\widetilde{v}_r'\right], \tag{31a,b}$$

using (30b) and (26).

3. Exact wave field at al radial distances

In the particular case of purely radial modes or cylindrical waves (Subsection 3.1) excluding axial propagation, the radial dependence in the AVE wave equation leads to a Gaussian hypergeometric differential equation (Subsection 3.2) specifying without further approximation the wave field in all space.

3.1. Particular case of purely radial modes

The wave equation (28) has four regular singularities: (i) on axis $r = 0$; (ii) at infinity $r = \infty$; (iii) for zero sound speed (32a) that is (16b)≡(17b) imaginary radius (32b),

$$c_0(r_s) = 0 : r_s = \pm\mathrm{i}\frac{c_{00}}{\Omega}\sqrt{\frac{2}{\gamma}} = \pm\mathrm{i}r_0; \tag{32a,b}$$

(iv) for zero (29a) that is at the critical layer (33a) at (21b) the radius (33b),

$$(\omega_*/k)^2 = [c_0(r_c)]^2 : r_c = \pm\frac{\sqrt{2/\gamma}}{\Omega}\sqrt{\frac{\omega_*^2}{k^2} - c_{00}^2} = \pm r_0\sqrt{\left(\frac{\omega_*}{c_{00}r}\right)^2 - 1}, \tag{33a,b}$$

where the adiabatic sound speed equals the phase speed based on the Doppler shifted frequency. A linear differential equation of second-order with four regular singularities is reducible to a Heun equation [70,71]. The simpler case of three regular singularities leads to the Gaussian hypergeometric differential equation [58–60]. The latter applies suppressing one singularity, e.g., the critical layer (33a,b) by setting the axial wavenumber to zero $k = 0$ so that $X = 1$ in (29a) and the singularity (33a,b) corresponding to $X = 0$ is excluded. This particular case corresponds to cylindrical acoustic-vortical-entropy waves depending only on the radius and time, and generalizes cylindrical acoustic waves [2,3,6,7].

If the axial wavenumber is not zero, the vanishing of (29a) introduces a critical layer in the AVE wave equation (28). The condition $X = 0$ corresponding to $\pm kc_0 = \omega_* = \omega - kU$ leads to a singularity of the wave equation similar to those that occur for adiabatic acoustic-shear [31–44] and acoustic-vortical [45–57] waves and will be addressed subsequently. The present paper concentrates on non-homentropic effects, in the simpler case of zero axial wavenumber (34a), that is neglecting axial dependence, when there is (21b) no Doppler shift (34b) and the coefficients of the wave equation (29a–c) simplify respectively to (34d–f),

$$k = 0, \quad \omega_* = \omega, \quad (c_0^2)' = \gamma\Omega^2 r, \quad X = 1 : A = c_0^2/r + (c_0^2)' = \gamma\Omega^2 r + c_0^2/r, \tag{34a-e}$$

$$B = \omega^2 - 5\Omega^2 + \left(\Omega^2 r + c_0^2/r\right)' = \omega^2 - 4\Omega^2 + \gamma\Omega^2 - c_0^2/r^2, \tag{34f}$$

where the radial dependence of the sound speed (16b) was used (34c). Thus the acoustic-vortical-entropy wave equation (28) for (34a–f) a cylindrical wave of frequency ω simplifies to

$$c_0^2\widetilde{v}_r'' + \left(\gamma\Omega^2 r + c_0^2/r\right)\widetilde{v}_r' + \left[\omega^2 + (\gamma - 4)\Omega^2 - c_0^2/r^2\right]\widetilde{v}_r = 0. \tag{35}$$

The first author is indebted to the referee of an earlier paper for the derivation of this particular form (35) of the more general wave equation (28); (29a-c). Substituting (17a) in the wave equation (35) leads to

$$r^2\left(1+r^2/r_0^2\right)\widetilde{v}_r''+r\left(1+3r^2/r_0^2\right)\widetilde{v}_r'+\left\{\left[(\omega/c_{00})^2+(1-8/\gamma)/r_0^2\right]r^2-1\right\}\widetilde{v}_r=0\,. \tag{36}$$

Using (34a) and (17a,b), the remaining wave variables are the azimuthal velocity (25b), mass density (30b), temperature (31a), entropy (25c) and pressure (26) perturbation spectra specified respectively by (37a–e),

$$\widetilde{v}_\varphi=-\mathrm{i}\frac{2\Omega}{\omega}\widetilde{v}_r,\quad \widetilde{\rho}=-\mathrm{i}(\rho_0/\omega)\left(\widetilde{v}_r'+\widetilde{v}_r/r\right),\quad \widetilde{T}/T_0=\left[(\gamma/c_0^2)\widetilde{p}-\widetilde{\rho}\right]/\rho_0, \tag{37a-c}$$

$$\widetilde{s}=-\mathrm{i}\frac{2}{\omega}\frac{C_V r\widetilde{v}_r}{r^2+r_0^2},\quad \widetilde{p}=-\mathrm{i}\frac{\rho_0\gamma\Omega^2}{2\omega}\left[\left(r+2r/\gamma+r_0^2/r\right)\widetilde{v}_r+\left(r^2+r_0^2\right)\widetilde{v}_r'\right], \tag{37d,e}$$

in terms of the radial velocity perturbation spectrum.

The adiabatic exponent for a perfect gas is given by (38b) where (38a) is the number of degrees of freedom of a molecule,

$$N=3,5,6\,:\,\gamma=1+\frac{2}{N}=\frac{5}{3},\frac{7}{5},\frac{4}{3}, \tag{38a,b}$$

namely: (i) three for monoatomic gas; (ii) five for a diatomic gas or polyatomic gas with molecules in a line; (iii) six for a three-dimensional polyatomic molecule. The ratio of the azimuthal velocity of the mean flow at the reference radius (17b) to the sound speed on axis given by

$$\frac{r_0\Omega}{c_{00}}=\sqrt{\frac{2}{\gamma}}=\sqrt{\frac{2N}{N+2}}=\sqrt{\frac{6}{5}},\sqrt{\frac{10}{7}},\sqrt{\frac{3}{2}}, \tag{39}$$

that is of order unity and plays the role of swirl Mach number at the axis, bearing in mind that the sound speed (17a,b) is not constant. Using the sound speed (17a) at the sonic radius (40a) leads to (40b),

$$c_0(r_0)=c_{00}\sqrt{2}\,:\,r_0\Omega=\frac{c_0(r_0)}{\sqrt{\gamma}}=\sqrt{RT_0(r_0)}=\overline{c}_0(r_0), \tag{40a,b}$$

showing that the sonic radius corresponds to azimuthal velocity equal to the isothermal sound speed, that is isothermal swirl Mach number unity. For purely acoustic waves in an homentropic medium without swirl, the Mach number should be based on the adiabatic sound speed; for purely vortical waves in an incompressible homentropic flow, the Mach number should be based on the isothermal sound speed. The coupling of sound with vorticity leaves for acoustic-vortical-entropy waves unclear which of the two sound speeds should be used or even a combination of them; the acoustic-vortical coupling to non-homentropic conditions could also possibly change the adiabatic or isothermal sound speeds. It turns out from the analysis that the singularity of the AVE wave equation occurs at the Mach number unity based on the azimuthal velocity of swirl and the isothermal sound speed, as would be the case for purely vortical modes. The singularities of the AVE wave equation for purely radial modes or cylindrical waves are, besides the axis $r=0$ and infinity $r=\infty$, the points (32b) on the imaginary axis $r_s=\pm\mathrm{i}r_0$ at a distance equal to the sonic radius (39). Thus there is no singularity of the AVE wave equation for real, finite, non-zero radius, and the wave field is finite everywhere, including at the sonic radius, that is r_s is an apparent singularity of the differential equation [66] for real variable that is not a singularity of the solution. Nevertheless, the singularities $|r_s|=r_0$ lie on a circle of radius r_0 in the complex r-plane and limit the radius of convergence of the solution around the axis. Other solutions will be used to cover the whole range of radial distances $0\le r<\infty$ including across the sonic radius $r=r_0$. This will be confirmed from the exact solution of the AVE wave equation, that has three regular singularities, and thus must be expressible in terms of Gaussian hypergeometric functions (Subsection 3.2).

3.2. Transformation to a Gaussian hypergeometric differential equation

The independent variable is chosen to be the square of the radius divided by the reference radius (41a),

$$\eta\equiv\frac{r^2}{r_0^2}=\frac{\Omega^2\gamma r^2}{2c_{00}^2}=\frac{\Omega^2\gamma r^2}{\left[c_0(r_0)\right]^2}=\frac{\Omega^2 r^2}{RT_0(r_0)},\quad \widetilde{v}_r(r,\omega)=J(\eta,\kappa), \tag{41a,b}$$

that is the square of the isothermal swirl Mach number, that is the square of the ratio of the swirl velocity to the isothermal sound speed. The acoustic-vortical-entropy wave equation (36) becomes

$$\eta^2(1+\eta)J''+\eta(1+2\eta)J'+[(\kappa^2\eta-1)/4]J=0, \tag{42}$$

that involves as parameter only the dimensionless radial wavenumber (43a,b), that includes all compressibility, vorticity and non-isentropic effects,

$$\kappa^2=\overline{\omega}^2+1-8/\gamma,\quad \overline{\omega}\equiv\omega r_0/c_{00}\,. \tag{43a,b}$$

The dimensionless radial wavenumber (43a) differs by constant terms from the dimensionless frequency or reference Helmholtz number (43b) calculated from: (i) the wave frequency ω; (ii) the sonic radius (39); (iii) the adiabatic sound speed on axis (16a).

The order of the polynomial coefficients may be reduced from cubics in the differential equation (42) to quadratic via the change of dependent variable (44a) in (42) leads to (44b),

$$J(\eta) = \eta^{\alpha} K(\eta) \ : \tag{44a}$$

$$\eta^2(1+\eta)K'' + \eta[1 + 2\alpha + 2(1+\alpha)\eta]K' + [(\alpha^2 + \alpha + \kappa^2/4)\eta + \alpha^2 - 1/4]K = 0, \tag{44b}$$

where the constant α may be chosen at will. Choosing (45a) allows (44b) to be divided through η, depressing the degree of the coefficients from three in (44b) to two in (45b),

$$\alpha = \frac{1}{2} \ : \ \eta(1+\eta)K'' + (2+3\eta)K' + [(\kappa^2+3)/4]K = 0\,. \tag{45a,b}$$

The differential equation (45b) is similar to the Gaussian hypergeometric type reversing the sign of the independent variable, that is using a change of independent variable (46a,b) that leads to (46c),

$$u = -\eta, \quad K(\eta) = Q(u) \ : \ u(1-u)Q'' + (2-3u)Q' - [(\kappa^2+3)/4]Q = 0\,. \tag{46a-c}$$

The latter is indeed a Gaussian hypergeometric differential equation [59],

$$u(1-u)Q'' + [C - (A+B+1)u]Q' - ABQ = 0, \tag{47}$$

with parameters satisfying (48a-c),

$$C = 2, \quad A + B = 2, \quad AB = \frac{\kappa^2+3}{4}, \tag{48a-c}$$

and implying (48d,e),

$$A, B = 1 \pm \frac{1}{2}\sqrt{1-\kappa^2} = 1 \pm \frac{\nu}{2}, \quad \nu \equiv \sqrt{1-\kappa^2}, \tag{48d,e}$$

where ν may be zero, real or imaginary respectively for $\kappa^2 = 1, \kappa^2 < 1$ and $\kappa^2 > 1$ in (43a,b). These three cases will be considered in the sequel.

The Gaussian hypergeometric differential equation (47) transforms into itself with different parameters by the changes of independent variable [58] in the Schwartz group,

$$u,\ 1-u,\ \frac{1}{u},\ 1-\frac{1}{u},\ \frac{u-1}{u},\ \frac{u}{u-1} \tag{49}$$

that interchange between themselves the three regular singularities: $u = 0, 1, \infty$. Since $\eta > 0$ in (41a) and $u < 0$ in (46a), the variable (50a) does not exceed unity,

$$\xi \equiv \frac{u}{u-1} = \frac{\eta}{\eta+1} = \frac{r^2}{r^2+r_0^2} < 1, \quad 0 \le r < \infty, \tag{50a,b}$$

and the corresponding series solution converges for (50b) that is for all finite values of the radius, including the origin and possibly excluding only the point at infinity since $\xi \to 1$ as $r \to \infty$. The solutions of the Gaussian hypergeometric differential equation in terms of the variable (50a) are [72]

$$Q_+(u) = (1-u)^{-A} F(A, C-B; C; u/(u-1)), \tag{51a}$$

$$Q_-(u) = u^{1-C}(1-u)^{C-A-1} F(A-C+1, 1-B; 2-C; u/(u-1))\,. \tag{51b}$$

Substituting (48a,d), (50a) and (46a,b; 45a; 44ba; 41a,b) leads to (52a,b) with $\widetilde{v}_{r\pm}$ corresponding to $Q_\pm(u)$ in (51a,b),

$$\widetilde{v}_{r+}(r,\omega) = \frac{r}{r_0}\left(\frac{r_0^2}{r_0^2+r^2}\right)^{1+\nu/2} F\left(1+\frac{\nu}{2}, 1+\frac{\nu}{2}; 2; \frac{r^2}{r_0^2+r^2}\right), \tag{52a}$$

$$\widetilde{v}_{r-}(r,\omega) = -\frac{r_0}{r}\left(\frac{r_0^2}{r_0^2+r^2}\right)^{\nu/2} G\left(\frac{\nu}{2}, \frac{\nu}{2}; 0; \frac{r^2}{r_0^2+r^2}\right), \tag{52b}$$

where a function of the second kind appears because the third parameter is zero in (52b). The radial velocity perturbation spectrum is a linear combination (53b) of (52a,b) with coefficients $C_\pm(\omega)$ that can depend on the frequency,

$$0 \le r < \infty \ : \ \widetilde{v}_r(r,\omega) = C_+\widetilde{v}_{r+}(r,\omega) + C_-\widetilde{v}_{r-}(r,\omega), \tag{53a,b}$$

that is valid for all values of the radius (50b) excluding only (53a) the asymptotic approximation at infinity that is discussed in the sequel.

The point at infinity (54a) corresponds (50a) to the point unity (54b) and the convergence of the Gaussian hypergeometric series (54c) at this point depends [18,73,74] on the value of (54d),

$$r \to \infty, \quad \xi \to 1, \quad F(a,b;c;\xi) \;:\; Y = Re(a+b-c)\,. \tag{54a-d}$$

The parameters of the Gaussian hypergeometric functions (52a,b) are respectively (55a,b) both leading to (55c),

$$\{a,b,c\} = \{1+\nu/2, 1+\nu/2, 2\}, \quad \{\nu/2, \nu/2, 0\} \;:\; Y = Re(\nu)\,. \tag{55a-c}$$

The parameter ν is given by (48a) implying that it is real (56b) for (56a) and imaginary (56d) for (56c),

$$0 \le \kappa^2 \le 1 \;:\; 1 \ge \nu \ge 0; \quad \kappa^2 > 1 \;:\; \nu = \pm i|\nu|\,. \tag{56a-d}$$

At the point unity $\xi = 1$ on the circle of convergence $|\xi| = 1$, the hypergeometric series has [18,73,74] the following properties: (i) diverges if $Y > 0$ that is if $\kappa^2 < 1$; (ii) also diverges if $a+b = c$ that implies by (55a,b) that $\nu = 0$ or $\kappa = 1$; (iii) oscillates for $Y = 0$ with $a+b \neq c$, that the case (56c,d); (iv) converges absolutely for $Y < 0$ that does not occur in the present case. Thus both solutions (52a,b) diverge (56a,b) or oscillate (56c,d) asymptotically (54a,b). The asymptotic solution for large radius will be obtained subsequently by analytic continuation using Gaussian hypergeometric functions of another variable from the Schwartz group (49). The AVE wave field (52b) is singular on the axis $r \to 0$ on account both of the factor r_0/r and the logarithmic singularity $\log[r^2/(r_0^2+r^2)]$ in the Gaussian hypergeometric function of the second kind [58]. Thus for a finite wave field on the axis, the second term on the r.h.s. of (53b) must be excluded for a cylindrical duct (57b) setting (57a) and leading to (57c),

$$C\_(\omega) = 0, 0 \le r < \infty \;: \tag{57a,b}$$

$$\tilde{v}_r(r,\omega) = C_+(\omega)(r/r_0)(1+r^2/r_0^2)^{-1-\nu/2} F\left(1+\frac{\nu}{2}, 1+\frac{\nu}{2}; 2; \frac{r^2}{r^2+r_0^2}\right). \tag{57c}$$

Using [58–60] the property (58a), it follows that the radial velocity perturbation spectrum vanishes on the axis (58b),

$$F(a,b;c;0) = 1 \;:\; \tilde{v}_r(0,\omega) = 0\,. \tag{58a,b}$$

The constant C_+ in (57c) is determined (59c) by the velocity perturbation spectrum at the sonic radius (59a,b),

$$r = r_0, \xi = \frac{1}{2} \;:\; \tilde{v}_r(r_0,\omega) = C_+(\omega) 2^{-1-\nu/2} F\left(1+\frac{\nu}{2}, 1+\frac{\nu}{2}; 2; \frac{1}{2}\right). \tag{59a-c}$$

The radial velocity perturbation spectrum (57c) vanishes on the axis as $O(r)$, that is the same as the azimuthal velocity $\Omega r \sim O(r)$ of the mean flow with rigid body swirl. Their ratio specifies the relative radial velocity perturbation spectrum (60b),

$$0 \le r < \infty \;: \tag{60a}$$

$$W_+(r,\omega) \equiv \frac{\tilde{v}_r(r,\omega)}{\Omega r} = \frac{C_+(\omega)}{\Omega r_0}(1+r/r_0)^{-1-\nu/2} F\left(1+\frac{\nu}{2}, 1+\frac{\nu}{2}; 2; \frac{r^2}{r^2+r_0^2}\right), \tag{60b}$$

that holds for finite radius (60a) and takes finite values on axis (61a) and at the sonic radius (61b),

$$W_+(0,\omega) = \frac{C_+(\omega)}{\Omega r_0}, \quad W_+(r_0,\omega) = W_+(0,\omega) 2^{-1-\nu/2} F\left(1+\frac{\nu}{2}, 1+\frac{\nu}{2}; 2; \frac{1}{2}\right). \tag{61a,b}$$

The asymptotic wave field is obtained next.

3.3. Wave fields inside, outside and at the sonic radius

Replacing the variable (50a) by (62a) would map all radial distances outside the origin up to and including infinity (62b) into the unit interval (62c),

$$\zeta \equiv \frac{r_0^2}{r_0^2+r^2} \;:\; 0 < r \le \infty \;:\; 0 \le \zeta < 1\,. \tag{62a-c}$$

The variable (50a) is mapped to (62a) by the transformation (63a) as can be confirmed from (63b),

$$\zeta = \left(1+\frac{r^2}{r_0^2}\right)^{-1} = \left(1+\frac{\xi}{1-\xi}\right)^{-1} = 1-\xi, \quad 1-\frac{r^2}{r^2+r_0^2} = \frac{r_0^2}{r^2+r_0^2}\,. \tag{63a,b}$$

The transformation (63a) belongs to the Schwartz group (49) and leads [72] from the hypergeometric function (54c) to

$$F(a,b;c,\xi)=\frac{\Gamma(c)\Gamma(c-a-b)}{\Gamma(c-a)\Gamma(c-b)}F(a,b;a+b-c+1;1-\xi)+ \\ +(1-\xi)^{c-a-b}\frac{\Gamma(c)\Gamma(a+b-c)}{\Gamma(a)\Gamma(b)}F(c-a,c-b;c-a-b+1;1-\xi)\,, \tag{64}$$

where Γ is the Gamma function [18,75]. Substituting (64) with the variable (63b) and parameters (55a) in the radial velocity perturbation spectrum (57c) that is non-singular at the origin leads to (65a,b)

$$0\le r<\infty\;:\;\tilde{v}_r(r,\omega)=C_+(\omega)\left[\tilde{v}_r^+(r,\omega)+\tilde{v}_r^-(r,\omega)\right], \tag{65a,b}$$

where

$$\tilde{v}_r^{\pm}(r,\omega)=\frac{1}{r/r_0+r_0/r}\left(\frac{r_0^2}{r^2+r_0^2}\right)^{\pm\nu/2}\frac{\Gamma(\pm\nu)}{[\Gamma(1\pm\nu)]^2} \\ F\left(1\pm\frac{\nu}{2},1\pm\frac{\nu}{2};1\pm\nu;\frac{r_0^2}{r_0^2+r^2}\right). \tag{66}$$

From (58a) follows the asymptotic limit for large radius,

$$\lim_{r\to\infty}\tilde{v}_r^{\pm}(r,\omega)=\left(\frac{r_0}{r}\right)^{1\pm\nu}\frac{\Gamma(\pm\nu)}{[\Gamma(1\pm\nu)]^2}. \tag{67}$$

From (48c) follows that in the case (56a,b) both solutions are asymptotically evanescent and non-oscillating (68a,b),

$$0\le\kappa^2\le 1\;:\;\lim_{r\to\infty}\tilde{v}_r^{\pm}(r,\omega)=0\,; \tag{68a,b}$$

from (56c,d) follows that for (69a) there are inward and outward propagating modes (69b) with decaying amplitude,

$$\kappa^2>1\;:\;\tilde{v}_r^{\pm}(r,\omega)\sim\frac{\Gamma(\pm i|\nu|)}{[\Gamma(1\pm i|\nu|)]^2}\frac{r_0}{r}\exp\left[\pm i|\nu|\log\left(\frac{r_0}{r}\right)\right]. \tag{69a,b}$$

At the origin (66) would vanish in agreement with (58b) provided that the hypergeometric series (70a) converges for $\zeta = 1$,

$$F\left(1\pm\frac{\nu}{2},1\pm\frac{\nu}{2};1\pm\nu;1\right)\;:\;\{a,b,c\}=\left\{1\pm\frac{\nu}{2},1\pm\frac{\nu}{2};1\pm\nu\right\},\quad a+b=c, \tag{70a-c}$$

the parameters (70b) lead to (70c), and thus [18,73,74] the hypergeometric series (70a) at the point $\zeta = 1$ on the radius of convergence $|\zeta| = 1$ diverges. Thus the conclusion (58b) cannot be drawn from the limit $0\times\infty$ in (66) as $r\to\infty$, although it can be proved from (57c).

Thus the finite wave field at the origin is given for the radial velocity perturbation spectrum: (i) by (57c) valid for all finite radial distances (57b); (ii) by (65b,66) for all radial distances including infinity and excluding the origin. The wave field vanishes at the origin (58b), where the relative wave field (60aa,b) is finite (61a). Both the absolute (57c) and relative (60b) radial velocity perturbation spectra are finite at the sonic radius taking respectively the values (59c) and (61b). The asymptotic radial velocity perturbation spectrum (67) decays both for monotonic (68a,b) and oscillating (69a,b) conditions. In the propagating case (69a,b) the modes (66) are complex conjugate (71a,b) implying (71c),

$$\kappa^2>1\;:\;\{\tilde{v}_r^-(r,\omega)\}^*=\tilde{v}_r^+(r,\omega)\;:\;\tilde{v}_r(r,\omega)=2C_+(\omega)\Re[\tilde{v}_r^+(r,\omega)]\,. \tag{71a-c}$$

Thus for real $C_+(\omega)$ the radial velocity perturbation spectrum,

$$\kappa^2>1\;:\;\tilde{v}_r^S(r,\omega)=\frac{2C_+(\omega)}{r/r_0+r_0/r}\Re\left\{\frac{\Gamma(\pm i|\nu|)}{[\Gamma(1\pm i|\nu|)]^2}F\left(1\pm i\frac{|\nu|}{2},1\pm i\frac{|\nu|}{2};1\pm i|\nu|;\frac{r_0^2}{r_0^2+r^2}\right)\exp\left[\pm i\frac{|\nu|}{2}\log\left(\frac{r_0^2}{r_0^2+r^2}\right)\right]\right\}, \tag{72}$$

corresponds to standing modes vanishing both on axis and at infinity,

$$\lim_{r\to 0}\tilde{v}_r^S(r,\omega)=0=\lim_{r\to\infty}\tilde{v}_r^S(r,\omega)\,. \tag{73a,b}$$

The application of rigid or impedance wall boundary conditions specifies the eigenvalues and eigenfunctions of AVE modes (Section 4).

4. Velocity, pressure, density, entropy and temperature perturbations

The solutions of the AVE wave equation are considered (Subsection 4.1) for a cylinder. The boundary conditions at the wall(s), e.g. rigid or impedance, specify the eigenvalues and eigenfunctions (Subsection 4.2) that are plotted for all wave variables (Subsection 4.3) over a range of radial distances including the sonic radius (Figs. 2–7).

4.1. AVE wave inside or outside a cylinder and in an annulus

All wave variables, namely the azimuthal velocity, mass density, pressure, temperature and entropy perturbations spectra can be calculated from the radial velocity perturbation spectrum (Section 2). The latter satisfies the acoustic-vortical-entropy wave equation whose solution has been obtained (Section 3) for all radial distances, including the predominantly acoustic modes inside and vortical modes outside the sonic radius where the isothermal swirl Mach number is unity and the radial velocity perturbation is finite, showing a smooth transition between the acoustically and vortically dominated propagation regimes. The calculation of eigenvalues and eigenfunctions is illustrated in the simplest case of a cylinder (74a) of radius R and the simplest boundary condition of a rigid wall (74b) leading (57c) to (74c),

$$0 \le r \le R\,, \; \tilde{v}_r(R,\omega) = 0 \;:\; F(1+\nu/2, 1+\nu/2; 2; R^2/(r_0^2+R^2)) = 0\,. \tag{74a-c}$$

The Gaussian hypergeometric function in (57c) can be calculated most efficiently [76,77] summing the series (75b,a) with the recurrence formula for the successive terms (75c) starting at (75b),

$$H(\xi;\nu) \equiv F(1+\nu/2, 1+\nu/2; 2; \xi) = 1 + \sum_{n=1}^{\infty} f_n(\xi), \tag{75a}$$

$$f_0(\xi) = 1, \quad f_{n+1}(\xi) = f_n(\xi)\frac{(n+1+\nu/2)^2}{(n+1)(n+2)}\xi\,. \tag{75b,c}$$

The eigenvalues for the radial wavenumber are the roots of (76),

$$0 = H\left(\frac{1}{1+(r_0/R)^2}; \sqrt{1-\kappa^2}\right) = H_0 \prod_{l=1}^{\infty}(\kappa - \kappa_l), \tag{76}$$

where H_0 is a constant. To each eigenvalue corresponds (57c) an eigenfunction,

$$\bar{v}_l(r/r_0) = (r/r_0)(1+r^2/r_0^2)^{-1-\nu/2} H\left(\frac{1}{1+(r_0/r)^2}; \sqrt{1-\kappa_l^2}\right)\,. \tag{77}$$

The eigenvalues κ_l for the radial wavenumber specify the eigenfrequency (43b) by (43a) with the adiabatic exponent $\gamma = 1.4$ for a diatomic perfect gas, and ν is given by (48e). Thus for (56a,b) the factor in (77) is real, whereas for (56c,d)≡(78a) there is an oscillating factor (78b),

$$\kappa^2 > 1 \quad |\nu| = |\kappa^2 - 1|^{1/2} \;: \tag{78a}$$

$$(1+r^2/r_0^2)^{-1-\nu/2} = (1+r^2/r_0^2)^{-1}\exp\left\{\mp i\frac{|\nu|}{2}\log(1+r^2/r_0^2)\right\}\,. \tag{78b}$$

Before proceeding to plot (Figs. 2–7) the eigenvalues and eigenfunctions for all variables (Subsections 4.2-4.3), the only parameter in the problem, namely the dimensionless wavenumber (43a) is interpreted in a simple way.

If the radius is small compared with the reference radius (79a), that is for small swirl isothermal Mach number, the wave equation (36) simplifies to (79b),

$$r^2 \ll r_0^2 \;:\; r^2\tilde{v}_r'' + r\tilde{v}_r' + \left(\kappa^2 r^2 - 1\right)\tilde{v}_r = 0, \tag{79a,b}$$

in the passage from (35) to (79b) the approximation (79a) was made in the coefficient of $\tilde{v}_r'$, but not in the coefficient of $\tilde{v}_r$, because the frequency (43b) could be large in the radial wavenumber (43a). Thus the approximation of small radius (79a) leads to the Bessel [61–63] equation (79b) where (43a) is the dimensionless radial wavenumber involving the dimensionless frequency (43b). The Bessel equation has oscillatory solutions for real wavenumber and monotonic increasing solutions for imaginary wavenumber. Although the preceding result was obtained only for small radius (79a), it suggests the following interpretation. The condition specifying wave fields with oscillatory dependence on the radius (80a) is expressed by (80b) in terms of the dimensionless frequency (43b),

$$\kappa^2 > 0 \;:\; \frac{\omega r_0}{c_{00}} > \sqrt{\frac{8}{\gamma} - 1} = \sqrt{\frac{7N-2}{N+2}} = \sqrt{\frac{19}{5}, \frac{33}{7}, 5}\,. \tag{80a,b}$$

Using (17b) the condition for radially oscillatory AVE waves is written in terms of the angular velocity,

$$\omega > \frac{c_{00}}{r_0}\sqrt{\frac{8}{\gamma} - 1} = \Omega\sqrt{\frac{\gamma}{2}\left(\frac{8}{\gamma} - 1\right)} = \Omega\sqrt{4 - \frac{\gamma}{2}} = \Omega\sqrt{\frac{7}{2} - \frac{1}{N}} = \Omega\sqrt{\frac{19}{6}, \frac{33}{10}, \frac{10}{3}}\,. \tag{81}$$

Using the sound speed (40a) at the reference radius the oscillatory condition (80b) becomes

$$\frac{\omega r_0}{c_0(r_0)} = \frac{\omega r_0}{c_{00}\sqrt{2}} > \sqrt{\frac{4}{\gamma} - \frac{1}{2}} = \sqrt{\frac{8-\gamma}{2\gamma}} = \sqrt{\frac{7N-2}{2N+4}} = \sqrt{\frac{19}{10}, \frac{33}{14}, \frac{5}{2}}\,. \tag{82}$$

Bearing in mind that the modulus of the vorticity is twice the angular velocity (12b) the oscillatory condition (81) becomes

$$\frac{\omega}{|\varpi|} = \frac{\omega}{2\Omega} > \sqrt{1-\frac{\gamma}{8}} = \sqrt{\frac{7}{8}-\frac{1}{4N}} = \sqrt{\frac{7N-2}{8N}} = \sqrt{\frac{19}{24},\frac{33}{40},\frac{5}{6}} \equiv \mu\,. \tag{83}$$

Of the four forms of the oscillatory condition (80b), (81), (82) and (83) the last is independent of the geometry and may be the most general: a vortical, non-homentropic flow has perturbations with oscillatory dependence on the radial distance if the frequency is larger than the maximum of the modulus of the peak vorticity ϖ multiplied by the factor μ in (83).

The solutions of the linearized equations of motion of a fluid may alternatively be interpreted as waves if the amplitude is finite or as unbounded motions if the amplitude diverges. For cylindrical AVE waves that depend only on radius and time, and are sinusoidal in time with constant frequency, unboundedness can be considered only in the radial direction. Asymptotically for large radius a 'wave' would have finite amplitude and an 'unbounded motion' would have diverging amplitude. Thus the oscillatory condition excluding monotonic growth of perturbations could be equivalent to a boundedness condition for the mean flow. This conjecture can be applied (Fig. 1) to the growth of combustion perturbations in a confined space: (i) if the natural frequencies exceed the product $\mu\varpi$ there is no growth (Fig. 1a), and only the fundamental frequency needs to be considered $\omega_1 > \mu\varpi$; (ii) if the fundamental frequency and other modes lie below $\mu\varpi$ those modes lead to growth (Fig. 1b). The passage from oscillatory to the monotonic case could be due to: (i) increasing the vorticity of the mean flow, e.g. to achieve better mixing for 'lean' fuel saving combustion; (ii) increasing the size of the enclosure, so that the natural frequencies reduce, and fall below $\mu\varpi$. The remark (i) agrees with the observation that lean combustion tends to be unstable; the remark (ii) agrees with the observation that larger rocket motors are more prone to large amplitude oscillations. The criterion for no growth

$$\omega_1 > \mu\varpi_{\max}, \quad \mu = 0.890, 0.908, 0.913, \tag{84a,b}$$

that the fundamental frequency must be larger than the modulus of the peak vorticity times the factor (83) can be tested for more complex geometries using numerical codes. Similar conditions were obtained before for the stability of an inviscid boundary layer [67,68] and for sound in vortical flows [69]. It has a simple interpretation: (i) acoustic modes with frequency ω are bounded; (ii) vortical modes with vorticity ϖ are unbounded; (iii) there is boundedness if the acoustic modes do not excite vortical modes $\omega > |\varpi|$; (iv) there is unboundedness if the vortical modes are excited by acoustic modes $\mu|\varpi| > \omega$. The factor (83) involving the adiabatic exponent appears because the vortical modes are incompressible and the acoustic modes are adiabatic and thus the ratio of frequency to vorticity is close to but not exactly unity bearing in mind the coupling with entropy effects.

The preceding results are comparable to the stability theory [78–81] in a spatial rather than a temporal domain; they hold for distance from the axis small compared with the sonic radius (79a), and are complemented by (77;78a,b) asymptotically for radial distance large compared with the sonic radius. In the latter case, the asmptotic scaling is specified by the dimensionless wavenumber (43a,b): (i) oscillatory for $\kappa^2 > 0$ and monotonic decaying or increasing for $\kappa^2 < 0$; (ii) real factor in (77) for $\kappa^2 \le 1$ and complex (78b) for (78a). The initial (57c) and asymptotic (53b,66) wave fields are valid for all radial distances except respectively infinity (57b) and the origin (53a) and thus overlap and can be matched for all radii except at these two points $0 < r < \infty$. The waveforms are not sinusoidal and thus an interpretation in terms of dimensionless wavenumber (43a) or frequency (43b) is local. For small radius compared with the sonic radius, the condition (80a) for oscillatory wave field leads to (85b), (81), (82) and (83) that are equivalent to (84a,b). In the opposite (85a) asymptotic limit (53a,b), the condition for oscillatory motion (85b) leads (43b) to (85c) for the frequency

$$r >> r_0 : \kappa^2 = \varpi^2 + 1 - 8/\gamma > 1, \quad \varpi > \sqrt{8/\gamma}\,. \tag{85a-c}$$

The condition (85c) is similar to (80b) with substitution (86a)

$$\sqrt{\frac{8}{\gamma}-1} \to \sqrt{\frac{8}{\gamma}}, \quad \frac{\omega}{\varpi} = \frac{c_{00}\varpi}{2\Omega r_0} = \frac{\varpi}{2}\sqrt{\frac{\gamma}{2}} > 1, \tag{86a,b}$$

and implies (86b) instead of (84a,b). Thus the factor (84b) for the initial wave field, that depends on the number of degrees of freedom of a molecule, is replaced asymptotically by (86b) implying $\omega > \varpi$ that does not depend on the atomic composition of

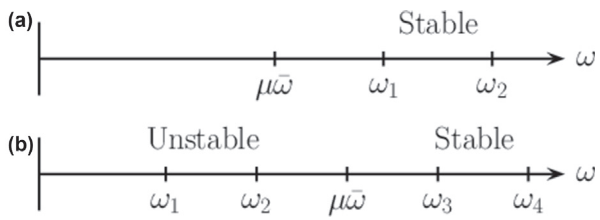

Fig. 1. The compressible, vortical, non-isentropic flow is oscillatory if the peak vorticity multiplied by (83) is less than the fundamental frequency (a) and monotonic otherwise (b).

a molecule of perfect gas. The spatial growth of acoustic-vortical perturbations [50,51] may appear an alternative to the temporal growth [52] as an indicator of instability. There is no restriction on the radius or frequency in the exact solutions (75a-c) for the eigenvalues (76) and eigenfunctions (77) that will be used for plotting the radial dependencies of all wave variables thus showing the boundedness or unboundedness of all acoustic-vortical-entropy wave modes.

4.2. Eigenvalues for the wavenumber and frequency and eigenfunctions for six wave variables

The AVE waves are considered inside a cylinder with radius (87a) for the four cases (87b),

$$0 \le r \le R : R/r_0 = 0.4, 0.8, 1.2, 1.6, \tag{87a,b}$$

of which the first (last) two do not (do) contain the sonic radius. For each cylinder the roots of (76) specify the first six eigenvalues κ_l of the radial wavenumber ordered by non-decreasing modulus in Table 1; the corresponding dimensionless natural frequencies $\overline{\omega}_l$ follow from (43b) and appear in Table 2. The eigenfunctions (77) are calculated from (75a-c) that converges (57c) for any finite value of the radius (57b) in a cylinder that may thus contain the sonic radius. To each pair of dimensionless eigenvalues $(\kappa_l, \overline{\omega}_l)$ correspond six dimensionless eigenfunctions for distinct wave variable spectra, namely the dimensionless: (i) radial velocity (77) with magnitude unity at the origin apart from the factor r/r_0,

$$D_l \equiv G\left(0; \sqrt{1-\kappa_l^2}\right) : \overline{v}_l(r/r_0) = \frac{\tilde{v}_r(r,\omega)}{D_l}, \tag{88a,b}$$

that is plotted in Fig. 2; (ii) azimuthal (37a) velocity (89),

$$\overline{w}_l(r/r_0) \equiv \frac{c_{00}}{\Omega r_0}\frac{\tilde{v}_\varphi(r,\omega)}{D_l} = -\mathrm{i}\frac{2}{\overline{\omega}_l}\overline{v}_l(r/r_0), \tag{89}$$

that is plotted in Fig. 3; (iii) the mass (37b) density (90),

$$\overline{\rho}_l(r/r_0) \equiv \frac{c_{00}}{D_l}\frac{\tilde{\rho}}{\rho_0} = -\frac{\mathrm{i}}{\overline{\omega}_l}[\overline{v}_l' + (r_0/r)\overline{v}_l], \tag{90}$$

that is plotted in Fig. 4; (iv) the (37d) entropy (91),

$$\overline{s}_l(r/r_0) \equiv \frac{c_{00}}{D_l}\frac{\tilde{s}(r,\omega)}{C_V} = -\frac{2\mathrm{i}}{\overline{\omega}_l}\frac{1}{r/r_0 + r_0/r}\overline{v}_l, \tag{91}$$

that is plotted in Fig. 5; (v) the (37e) pressure (92),

$$\overline{p}_l(r/r_0) \equiv \frac{\tilde{p}(r,\omega)}{\rho_0 c_{00} D_l} = -\frac{\mathrm{i}}{\overline{\omega}_l}\left\{\left[(1+2/\gamma)\,r/r_0 + r_0/r\right]\overline{v}_l + \left(1 + r^2/r_0^2\right)\overline{v}_l'\right\}, \tag{92}$$

that is plotted in Fig. 6.

The temperature perturbation (37c) follows (94) from those of the density (90) and pressure (92),

Table 1
First six eigenvalues of the radial wavenumber for acoustic-vortical-entropy waves in a cylinder $0 \le r \le r_1$ with rigid wall with radius r_1 smaller or larger than the sonic radius r_0.

$0 \le r \le r_1$	$r_1 = 0.4r_0$	$r_1 = 0.8r_0$	$r_1 = 1.2r_0$	$r_1 = 1.6r_0$
κ_1	9.874	5.322	3.895	3.217
κ_2	18.015	9.626	6.974	5.700
κ_3	26.103	13.920	10.061	8.203
κ_4	34.175	18.212	13.150	10.712
κ_5	42.240	22.502	16.241	13.027 ± i14.338
κ_6	50.302	26.791	18.195 ± i27.868	15.588 ± i7.640

Table 2
As Table 1 for the corresponding values of the dimensionless frequency.

$0 \le r \le r_1$	$r_1 = 0.4r_0$	$r_1 = 0.8r_0$	$r_1 = 1.2r_0$	$r_1 = 1.6r_0$
$\overline{\omega}_1$	10.110	5.748	4.460	3.881
$\overline{\omega}_2$	18.145	9.868	7.304	6.100
$\overline{\omega}_3$	26.193	14.089	10.293	8.485
$\overline{\omega}_4$	34.244	18.341	13.329	10.930
$\overline{\omega}_5$	42.296	22.606	16.386	13.109 ± i14.248
$\overline{\omega}_6$	50.349	26.879	18.234 ± i27.809	15.710 ± i7.581

$$\overline{T}_l(r/r_0) \equiv \frac{c_{00}}{D_l}\frac{\widetilde{T}(r,\omega)}{T_0} = \frac{c_{00}}{\rho_0 D_l}\left[\gamma\frac{\widetilde{p}(r,\omega)}{[c_0(r)]^2} - \widetilde{\rho}(r,\omega)\right] = \tag{93}$$
$$= \frac{\gamma c_{00}^2}{[c_0(r)]^2}\overline{p}_l(r/r_0) - \overline{\rho}_l(r/r_0) = \frac{r_0^2}{2r^2}[M(r)]^2\overline{p}_l(r/r_0) - \overline{\rho}_l(r/r_0),$$

that is plotted in Fig. 7. It involves the isothermal swirl Mach number,

$$\gamma\frac{c_{00}^2}{[c_0(r)]^2} = \frac{\gamma^2\Omega^2 r_0^2}{2[c_0(r)]^2} = \frac{r_0^2}{2r^2}\frac{\gamma^2\Omega^2 r^2}{[c_0(r)]^2} = \frac{r_0^2}{2r^2}\frac{\Omega^2 r^2}{RT_0} = \frac{r_0^2}{2r^2}[M(r)]^2, \tag{94}$$

where were used (17a,b). In (90) and (92) appear the derivative with regard to its argument (95) of the radial velocity (88b),

$$\overline{v}'_l(r/r_0) \equiv \frac{\mathrm{d}[\overline{v}_r(r,\omega)]}{\mathrm{d}(r/r_0)}$$
$$= \frac{\mathrm{d}}{\mathrm{d}(r/r_0)}\left[\frac{r}{r_0}\left(1+\frac{r^2}{r_0^2}\right)^{-1-\nu/2} F\left(1+\frac{\nu}{2}, 1+\frac{\nu}{2}; 2; \frac{r^2}{r_0^2+r^2}\right)\right]$$
$$= \left(1+\frac{r^2}{r_0^2}\right)^{-2-\nu/2}\left\{\left[1-(1+\nu)\frac{r^2}{r_0^2}\right]F\left(1+\frac{\nu}{2}, 1+\frac{\nu}{2}; 2; \frac{r^2}{r_0^2+r^2}\right)\right.$$
$$\left. + \left(1+\frac{r^2}{r_0^2}\right)\left(\frac{1+\nu/2}{r/r_0+r_0/r}\right)^2 F\left(2+\frac{\nu}{2}, 2+\frac{\nu}{2}; 3; \frac{r^2}{r_0^2+r^2}\right)\right\}, \tag{95}$$

where was used (96a) the derivative (96b) of the Gaussian hypergeometric function in (75b,a),

$$\frac{\mathrm{d}\xi}{\mathrm{d}(r/r_0)} = \frac{2r_0^3 r}{(r_0^2+r^2)^2}, \tag{96a}$$

$$\frac{\mathrm{d}}{\mathrm{d}\xi}\left[F(1+\nu/2, 1+\nu/2; 2; \xi)\right] = \frac{(1+\nu/2)^2}{2}F(2+\nu/2, 2+\nu/2; 3; \xi). \tag{96b}$$

The Gaussian hypergeometric series in (96b) is calculated as (75a–c) replacing ν by $1+\nu$. The fundamental and first five harmonics are plotted in Figs. 2–7 respectively for the dimensionless radial (88a,b) and azimuthal (89) velocity, mass density (90),

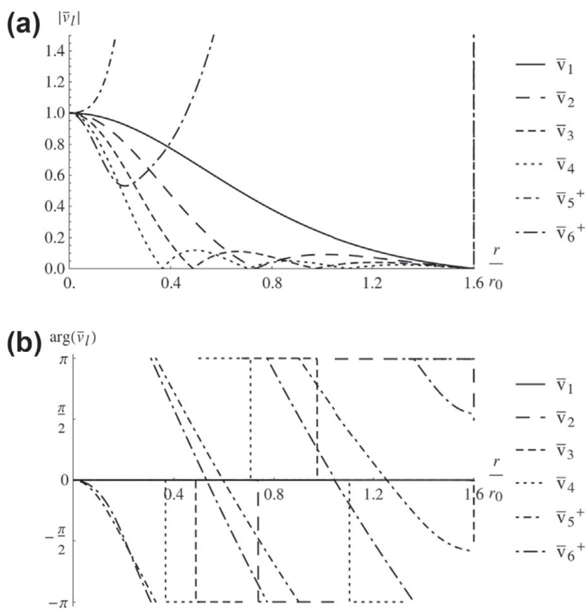

Fig. 2. Modulus (a) and phase (b) versus radial distance normalized to the sonic radius, for dimensionless radial velocity perturbation spectrum, of the first six modes of acoustic-vortical-entropy waves in a rigid cylinder with radius equal to 1.6 of the sonic radius.

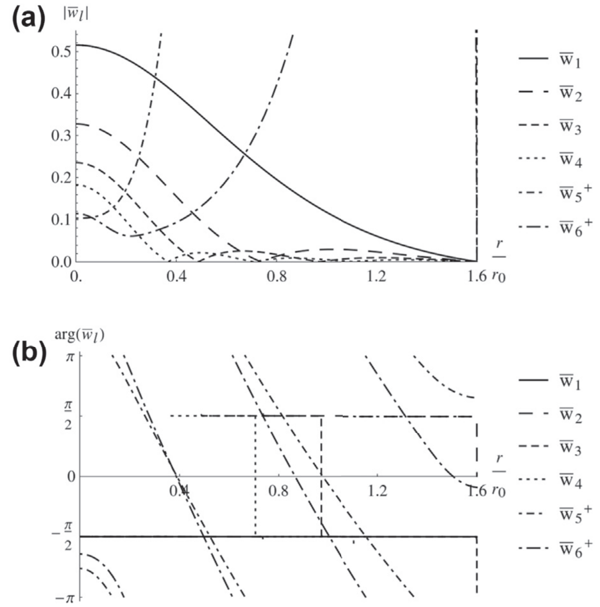

Fig. 3. Modulus (a) and phase (b) versus radial distance normalized to the sonic radius, for dimensionless azimuthal velocity perturbation spectrum, of the first six modes of acoustic-vortical-entropy waves in a rigid cylinder with radius equal to 1.6 of the sonic radius.

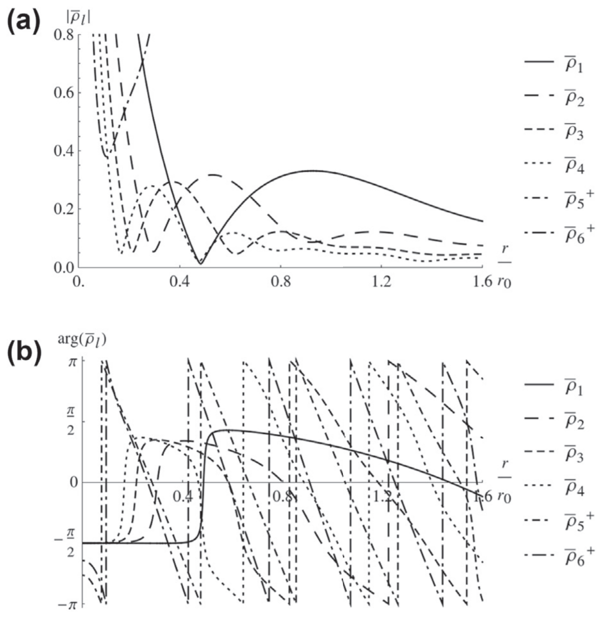

Fig. 4. Modulus (a) and phase (b) versus radial distance normalized to the sonic radius, for dimensionless mass density perturbation spectrum, of the first six modes of acoustic-vortical-entropy waves in a rigid cylinder with radius equal to 1.6 of the sonic radius.

entropy (91), pressure (92) and temperature (94) perturbation spectra, as basis for the following discussion (Subsection 4.3). The radius of the cylindrical duct is taken as the largest $R/r_0 = 1.6$ of the values in (87b) to show the variation of the AVE wave variables across the sonic radius.

4.3. Waveforms for the fundamental and stable and unstable harmonics

Figs. 2–7 concern AVE wavemodes in a cylindrical duct with rigid wall at a radius $R = 1.6r_0$ that is 60% larger than the sonic

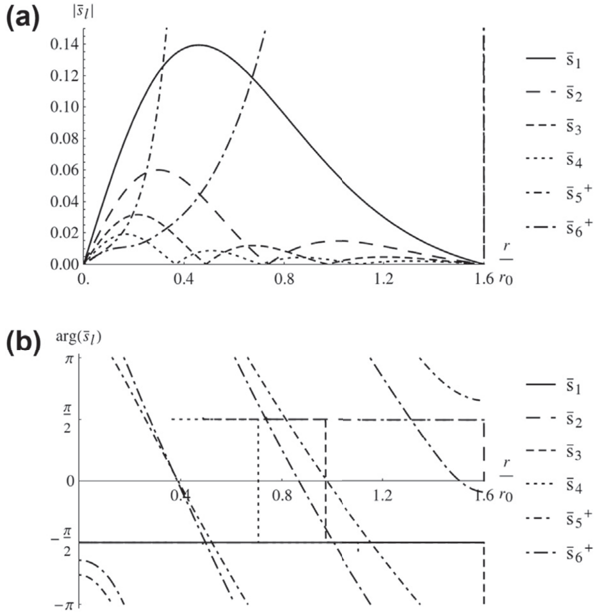

Fig. 5. Modulus (a) and phase (b) versus radial distance normalized to the sonic radius, for dimensionless entropy perturbation spectrum, of the first six modes of acoustic-vortical-entropy waves in a rigid cylinder with radius equal to 1.6 of the sonic radius.

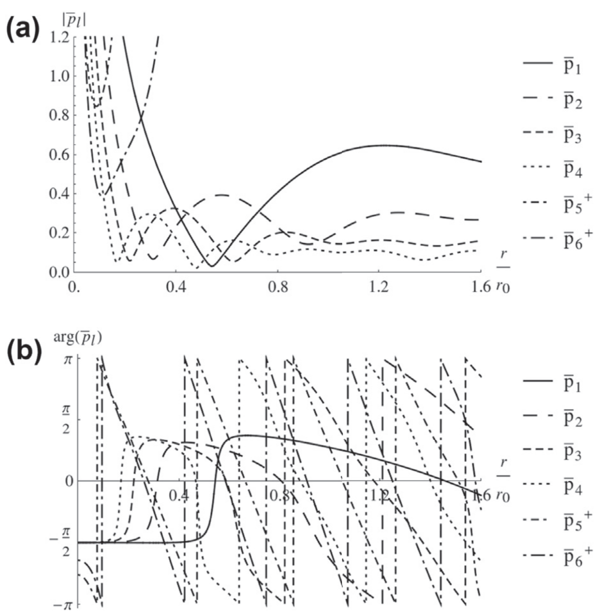

Fig. 6. Modulus (a) and phase (b) versus radial distance normalized to the sonic radius, for dimensionless pressure perturbation spectrum, of the first six modes of acoustic-vortical-entropy waves in a rigid cylinder with radius equal to 1.6 of the sonic radius.

radius, thus containing in its interior the radius of isothermal swirl Mach number unity, with subsonic (supersonic) swirl inside (outside). Since the mean flow has a solenoidal (13b) velocity (12a), it causes no compression in a compressible fluid that can support sound waves, and thus there is no restriction on Mach number. The first six modes are considered with dimensionless frequency (43b) indicated in Table 2, with the corresponding dimensionless radial wavenumbers (43a) in Table 1. The modulus and phase of the six corresponding eigenfunctions are plotted versus radial distance in Fig. 2 for the radial velocity (88b), in Fig. 3 for the azimuthal velocity (89), in Fig. 4 for the mass density (90), in Fig. 5 for the entropy (91), in Fig. 6 for the pressure (92) and in Fig. 7 for the temperature (93); for all six wave variables are considered as dimensionless perturbation spectra using the amplitude D_l of the radial velocity perturbation spectrum at the axis. For this reason, the waveforms or eigenfunctions for

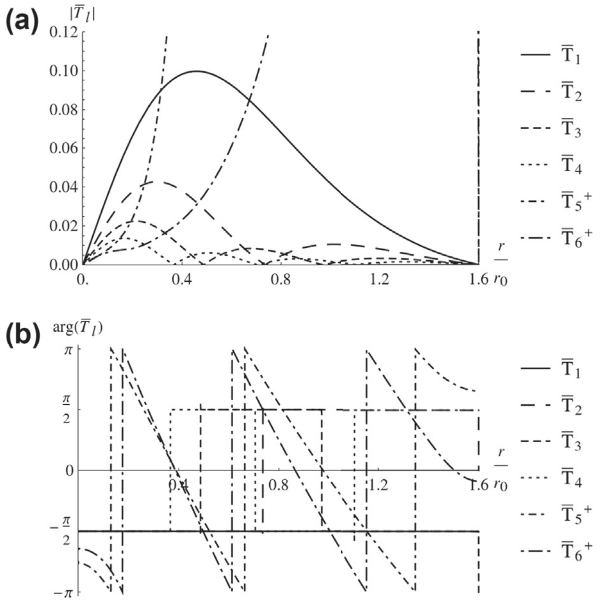

Fig. 7. Modulus (a) and phase (b) versus radial distance normalized to the sonic radius, for dimensionless temperature perturbation spectrum, of the first six modes of acoustic-vortical-entropy waves in a rigid cylinder with radius equal to 1.6 of the sonic radius.

the radial velocity start with the value unity on the axis in Fig. 2.

The dimensionless radial velocity perturbation spectra in Fig. 2 all start with the value unity on axis due to the normalization and all finish with zero at the rigid wall at $r = 1.6r_0 = R$. The fundamental mode $\overline{v}_1$ has no other zero, and decays smoothly from the axis to the wall. As typical of eigenvalue problems, the harmonics $\overline{v}_n$ of order $n = 2, 3, 4$ have $n-1$ zeros of the amplitude (Fig. 2 top) between the axis and the wall, corresponding to phase jumps of π (Fig. 2 bottom). The fifth and sixth harmonics $n = 5, 6$ have complex radial wavenumbers in Table 1, leading to radially decaying or divergent modes; the divergent modes are unbounded perturbations of the mean flow as can be seen from the increasing amplitudes of $\overline{v}_5^+$ and $\overline{v}_6^+$ (Fig. 2 top). The dimensionless azimuthal velocity perturbation spectrum (Fig. 3) also vanishes at the rigid wall for the fundamental $\overline{w}_1$ and next three harmonics $\overline{w}_2, \overline{w}_3, \overline{w}_4$ (Fig. 3 top), again with phase jumps of π at the zeros of the amplitude or nodes (Fig. 3 bottom). The fifth and sixth harmonics $\overline{w}_5^+, \overline{w}_6^+$ are unbounded modes both for the radial (Fig. 2 top) and azimuthal (Fig. 3 top) velocity perturbations spectra. The amplitude of the dimensionless azimuthal velocity perturbation spectrum on axis (Fig. 3 top) decreases from the fundamental to the higher harmonics.

The perturbation spectrum of the mass density (Fig. 4) leads to eigenfunctions that are quite different from those of the radial (Fig. 2) and azimuthal (Fig. 3) velocity perturbation spectra. The mass density perturbation spectra do not vanish at the rigid wall (Fig. 4 top) although their magnitude decreases from the fundamental $\overline{\rho}_1$ to the next three bounded harmonics $\overline{\rho}_2, \overline{\rho}_3, \overline{\rho}_4$. The fundamental $\overline{\rho}_1$ almost vanishes at $r = 0.48r_0$ leading to rapid phase change of π (Fig. 4 bottom). Whereas the fundamental $\overline{\rho}_1$ has one dip, the next three $n = 2, 3, 4$ harmonics $\overline{\rho}_n$ have n dips, and the fifth and sixth harmonics $\overline{\rho}_5^+, \overline{\rho}_6^+$ are unbounded as before. The dimensionless entropy perturbation spectrum (Fig. 5) vanishes on axis for all harmonics, including the unbounded harmonics $\overline{s}_5^+, \overline{s}_6^+$, and vanishes also at the rigid wall for the fundamental $\overline{s}_1$ and the first three bounded harmonics $\overline{s}_2, \overline{s}_3, \overline{s}_4$. The fundamental $\overline{s}_1$ has no zeros and exhibits a single peak at $r = 0.5r_0$ far from the sonic radius. The first three harmonics $\overline{s}_n$ with $n = 2, 3, 4$ have n peaks and $n-1$ nodes. The peaks are lower when: (i) passing from the fundamental $n = 1$ to the harmonics $n = 2, 3, 4$; (ii) for a given harmonic n, the successive n peaks become lower farther from the axis.

The dimensionless pressure perturbation spectra (Fig. 6) are broadly similar to those of the mass density (Fig. 4), with similar features, such as a non-zero pressure at the rigid wall with amplitude decreasing from the fundamental $\overline{p}_1$ to the first three bounded harmonics $\overline{p}_2, \overline{p}_3, \overline{p}_4$. The fifth and sixth harmonics $\overline{p}_5^+, \overline{p}_6^+$ are again unbounded. The fundamental $\overline{p}_1$ has one dip of the amplitude (Fig. 6 top) broader than for the mass density (Fig. 4 top) and approximately at the same location $r = 0.48r_0$. The next three bounded harmonics $\overline{p}_n$ with $n = 2, 3, 4$ have n dips and n peaks (Fig. 6 top) with phase jumps (Fig. 6 bottom) indicating that the dips are actually zeros or nodes. The dimensionless temperature perturbation spectra (Fig. 7) have eigenfunctions broadly similar to the entropy (Fig. 5), with: (i) zero on axis for all modes, bounded $\overline{T}_1, \overline{T}_2, \overline{T}_3, \overline{T}_4$ or unbounded $\overline{T}_5^+, \overline{T}_6^+$; (ii) the bounded modes are also zero at the wall; (iii) the fundamental mode $\overline{T}_1$ has a single maximum between the axis and the wall; (iv) the bounded harmonics $n = 2, 3, 4$ have n maxima and $n - 1$ zeros.

Thus besides the unbounded diverging spectra, there are three kinds of bounded spectra for the fundamental mode $n = 1$ (first three harmonics $n = 2, 3, 4$): (i) monotonic (oscillatory) decay for the dimensionless radial (Fig. 2) and azimuthal (Fig. 3) velocity perturbation spectra, that are non-zero on axis and zero at the wall; (ii) non-zero at the wall for the dimensionless mass density (Fig. 4) and pressure (Fig. 6) perturbation spectra with a single dip (n dips and $n - 1$ maxima); (iii) zero on axis and at the wall for the dimensionless entropy (Fig. 5) and temperature (Fig. 7) perturbation spectra with a single maximum (n maxima and $n - 1$ zeros).

5. Conclusions

The consideration of entropy modes requires that the equation of state (6a) following the motion be written as

$$\frac{DP}{dt} = c^2 \frac{d\Gamma}{dt} + \beta \frac{dS}{dt}, \tag{97}$$

involving both the adiabatic sound speed (6b) and the non-adiabatic coefficient (6c). For the mean state (97) simplifies to

$$\frac{\delta p_0}{dt} = c_0^2 \frac{\delta \rho_0}{dt} + \beta_0 \frac{\delta s_0}{dt}, \tag{98}$$

where the exact material derivative (5a,b) is replaced by the form (13a) for the mean flow. Subtracting (98) from (97) and linearizing leads to the perturbation equation

$$\frac{\delta p}{dt} + \boldsymbol{v} \cdot \nabla p_0 = c_0^2 \left(\frac{\delta \rho}{dt} + \boldsymbol{v} \cdot \nabla \rho_0 \right) + \beta_0 \left(\frac{\delta s}{dt} + \boldsymbol{v} \cdot \nabla s_0 \right), \tag{99}$$

where $\boldsymbol{v}$ is the velocity perturbation. Thus, to allow for the existence of entropy modes, the second terms on the r.h.s. of (98) and (99) should be considered, corresponding to non-adiabatic perturbations of a non-homentropic mean flow. For non-dissipative total flow (3), the second term on the r.h.s. of (97) can be omitted; for an isentropic mean flow (23a), this leads to entropy perturbations (24b) if the mean flow is non-homentropic.

The omission of the second terms on the r.h.s. of (97–99) in most of the literature on waves in fluid implies the exclusion of entropy modes. For example, the assumptions of homentropic mean flow and adiabatic perturbations in the presence of axisymmetric shear and swirl with arbitrary radial dependence [30,45,49–56] lead to acoustic-vortical waves, rather than acoustic-vortical-entropy waves [57]. There is not much additional literature concerning non-adiabatic waves. An exception is the consideration of waves in an homenergetic (rather than isentropic) shear flow with a linear velocity profile [41,42]. In the present paper, the vorticity of the mean flow is associated with swirl rather than shear. The entropy effects appear for internal waves, for example in a stable stratified atmosphere that is not an homentropic medium. In the case of acoustic-gravity waves [9,82–84], the stratification relates to gravity, unlike the present case of interaction of acoustic-entropy modes with a swirling flow. The assumptions of uniform axial flow and rigid body swirl imply that the velocity is a solenoidal vector, and causes no compression; hence there is no restriction on the Mach number and the first term on the r.h.s. of (98) can be omitted, relating pressure and entropy changes in the mean flow. For a compressible fluid, the compressions are entirely due to the wave perturbations. For constant mean flow mass density, the first term on the r.h.s of (99) is simplified. With these simplifications, the mean flow remains non-homentropic and the entropy perturbations also remain and interact with sound and vorticity.

In the present paper is derived a scalar wave equation with a single variable combining the interactions of the three types of waves in a fluid not subject to external force fields, hence the designation acoustic-vortical-entropy (AVE) waves. A deliberate choice was made of one of the simplest baseline flows that could support AVE waves, namely the non-dissipative, non-homentropic uniform flow with rigid body swirl of a perfect gas with constant density, leading to a mean flow pressure and sound speed varying radially due to the centrifugal force. The linear compressive perturbation of this mean flow leads in the axisymmetric case to the AVE wave equation (28); (29a-c) that is of the second-order. The extension to non-axisymmetric modes is known for acoustic-vortical waves [30,49,53–56] and acoustical-vortical-entropy waves [57] leading to a sixth-order wave equation whose analytical solution requires approximations such as the WKB limit of high-frequency leading to a second-order differential equation. In the axisymmetric case, the AVE wave equation can be solved exactly, and simplifies further for zero axial wave number, corresponding to cylindrical waves. Nothing is implied on whether the non-axisymmetric modes of AVE waves would be cut-off or cut-on. Thus the extension from acoustic cylindrical waves specified by Bessel functions to cylindrical acoustic-vortical-entropy waves leads to exact solutions in terms of Gaussian hypergeometric functions. This result may be of some fundamental interest, and may also serve as an original simplified model which could be used to validate a simplified numerical simulation. The six wave variables in this case are the frequency spectra of the perturbations of the (i) radial and (ii) azimuthal velocity, (iii) mass density, (iv) entropy, (v) pressure and (vi) temperature.

An important feature of the problem is the existence of a sonic radius where the swirl velocity equals the isothermal sound speed. It is shown that this condition of isothermal swirl Mach number unity corresponds to a finite wave field, and is neither a singularity of the AVE wave equation nor a singularity of the wave field. The singularity of the wave equation outside the origin and infinity occurs for imaginary radius and limits the radius of convergence of some solutions: this does not prevent the use of analytic continuation to obtain exact solutions valid for all radial distances and frequencies. The linear non-dissipative compressible vortical perturbations of the non-isentropic uniform flow with rigid swirl may be interpreted alternatively as (i) acoustic-vortical entropy (AVE) waves or (ii) radially bounded or unbounded modes of the mean flow. This dual interpretation is demonstrated for a cylindrical duct with rigid wall at the radius $a = 1.6 r_0$, that is 60% larger than the sonic radius, for: (a) the eigenvalues for the wavenumber (Table 1) and frequency (Table 2); (b) the eigenfunctions for the radial (Fig. 2) and azimuthal (Fig. 3) velocity, mass density (Fig. 4), entropy (Fig. 5), pressure (Fig. 6) and temperature (Fig. 7). These confirm that the wave field is finite at the sonic radius in this as well as in all other cases; in this particular case, the fundamental and first three harmonics are bounded and the fifth and sixth harmonics are unbounded. The general theory applies to all cases of cylindrical or annular ducts or cylindrical cavities containing or not the sonic radius.

The analysis could be extended from the wave equation (35) with zero axial wavenumber to the wave equation (28); (29a-c) allowing for axial propagation; the non-zero axial wavenumber leads to an additional propagating variable, namely the axial velocity perturbation. The wave equation has two additional singularities (100a) for (100b):

$$X = 0 : \pm c_0 k = \omega_*, \quad \omega = k[U \pm c_0(r)], \tag{100a-c}$$

corresponding (100c) to an axial phase velocity ω/k equal to the group velocity for axial propagation in the positive or negative z-direction. The additional extension to non-axisymmetric or spinning AVE waves would modify the linearized Euler equation (22fa-f) complicating the elimination for a scalar wave equation in one variable. The condition of oscillating motion, of frequency exceeding the vorticity in the far-field (86b) or (84a,b) in the near field could be modified by dissipative effects, like shear viscosity or thermal conductivity, not considered here. The rigid wall boundary condition (74b) could be replaced by impedance boundary conditions leading to other waveforms besides Figs. 2–7. These additional aspects are all worthy of consideration, and beyond the scope of the present paper, aimed at obtaining the simplest scalar acoustic-vortical-entropy wave equation for cylindrical modes and its exact solution in all space-time. The next step could be to allow for axial propagation described by the AVE wave equation (28;29a-c).

Acknowledgements

This work was supported by FCT (Foundation for Science and Technology), Portugal, through IDMEC (Institute of Mechanical Engineering), under LAETA, project UID/EMS/50022/2013.

Appendix A. Supplementary data

Supplementary data related to this article can be found at https://doi.org/10.1016/j.jsv.2018.09.017.

References

[1] L.S.G. Kovasznay, Turbulence in supersonic flow, J. Aero. Sci. 20 (10) (1953) 657–674.
[2] L.D. Landau, E.M. Lifshitz, Fluid Mechanics, Vol. 6 of Course of Theoretical Physics, Pergamon Press, 1959. ISBN:9780080091044.
[3] A.D. Pierce, Acoustics: an Introduction to its Physical Principles and Applications, McGraw-Hill, 1981. ISBN:9780883186121.
[4] L.M.B.C. Campos, On the generation and radiation of magneto-acoustic waves, J. Fluid Mech. 81 (3) (1977) 529–549, https://doi.org/10.1017/S0022112077002213.
[5] L.M.B.C. Campos, On magnetoacoustic-gravity-inertial (MAGI) waves – I. generation, propagation, dissipation and radiation, Mon. Not. Roy. Astron. Soc. 410 (2) (2011) 717–734, https://doi.org/10.1111/j.1365-2966.2010.17553.x.
[6] J.W.S. Rayleigh, The Theory of Sound, 2nd Edition, Vol. 2 Vols. Of Dover Books on Physics. (reprint), Dover Publications, 1945, p. 1877. ISBN:9780486602929.
[7] P.M. Morse, K.U. Ingard, Theoretical Acoustics, McGraw-Hill, 1968. ISBN:0691084254.
[8] M.E. Goldstein, Aeroacoustics, McGraw-Hill, 1976. ISBN:9780070236851.
[9] M.J. Lighthill, Waves in Fluids, Cambridge Mathematical Library, Cambridge U.P., 1978. ISBN:9780521010450.
[10] A.P. Dowling, J.E. Ffowcs-Williams, Sound and Sources of Sound, Ellis Horwood, 1983. ISBN:9780853125273.
[11] T.D. Rossing (Ed.), Handbook of Acoustics, Springer handbooks, Springer, 2007, ISBN:9780387336336.
[12] M.J. Crocker (Ed.), Handbook of Noise and Vibration Control, Wiley, 2007, ISBN:9780471395997.
[13] L.M.B.C. Campos, Generalized Calculus with Applications to Matter and Forces, Vol. 3 of Mathematics and Physics in Science and Engineering, CRC Press, 2014. ISBN: 9781420071153.
[14] H. Lamb, Hydrodynamics, fifth ed., Cambridge Mathematical Library, Cambridge U.P., 1932. ISBN:0521055156.
[15] L.M. Milne-Thomson, Theoretical Hydrodynamics, Dover, 1968. ISBN:0486689700.
[16] M.J. Lighthill, An Informal Introduction to Theoretical Fluid Mechanics, Institute of Mathematics & its Applications Monograph Series, Cambridge U.P., 1988. ISBN:9780198536307.
[17] M.S. Howe, Hydrodynamics and Sound, Cambridge U.P., 2006. ISBN:9780521868624.
[18] L.M.B.C. Campos, Complex Analysis with Applications to Flows and Fields, Vol. 1 of Mathematics and Physics in Science and Engineering, CRC Press, 2010. ISBN:9781420071184.
[19] M.S. Howe, Contributions to the theory of aerodynamic sound, with application to excess jet noise and the theory of the flute, J. Fluid Mech. 71 (5) (1975) 625–673, https://doi.org/10.1017/S0022112075002777.
[20] L.M.B.C. Campos, On the emission of sound by an ionized inhomogeneity, Proceed. Roy. Soc. Lond. Math. 359 (1696) (1978) 65–91, https://doi.org/10.1098/rspa.1978.0032.
[21] L.M.B.C. Campos, F.J.P. Lau, On sound generation by moving surfaces and convected sources in a flow, Int. J. Aeroacoustics 11 (1) (2012) 103–136, https://doi.org/10.1260/1475-472X.11.1.103.
[22] L.M.B.C. Campos, On linear and non-linear wave equations for the acoustics of high-speed potential flows, J. Sound Vib. 110 (1) (1986) 41–57, https://doi.org/10.1016/S0022-460X(86)80072-4.
[23] L.M.B.C. Campos, On waves in gases. part I: acoustics of jets, turbulence, and ducts, Rev. Mod. Phys. 58 (1) (1986) 117–182, https://doi.org/10.1103/RevModPhys.58.117.
[24] L.M.B.C. Campos, On the generalizations of the Doppler factor, local frequency, wave invariant and group velocity, Wave Motion 10 (3) (1988) 193–207, https://doi.org/10.1016/0165-2125(88)90018-2.
[25] W. Haurwitz, Zur theorie der wellenbewegungen in luft und wasser ("on the theory of wave perturbations in a flow in air and water"), Veröffentlichungen des Geophysikalischen Instituts der Karl-Marx-Universität Leipzig 6 (1) (1931) 334–364.
[26] D. Küchemann, Störungsbewegungen in einer gasströmung mit grenzschicht, Z. Angew. Math. Mech. 18 (4) (1938) 207–222, https://doi.org/10.1002/zamm.19380180402.
[27] D.C. Pridmore-Brown, Sound propagation in a fluid flowing through an attenuating duct, J. Fluid Mech. 4 (4) (1958) 393–406, https://doi.org/10.1017/S0022112058000537.

[28] W. Möhring, E. Müller, F. Obermeier, Problems in flow acoustics, Rev. Mod. Phys. 55 (3) (1983) 707–724, https://doi.org/10.1103/RevModPhys.55.707.
[29] L.M.B.C. Campos, On 36 forms of the acoustic wave equation in potential flows and inhomogeneous media, Appl. Mech. Rev. 60 (4) (2007) 149–171, https://doi.org/10.1115/1.2750670.
[30] L.M.B.C. Campos, On 24 forms of the acoustic wave equation in vortical flows and dissipative media, Appl. Mech. Rev. 60 (6) (2007) 291–315, https://doi.org/10.1115/1.2804329.
[31] M. Goldstein, E. Rice, Effect of shear on duct wall impedance, J. Sound Vib. 30 (1) (1973) 79–84, https://doi.org/10.1016/S0022-460X(73)80051-3.
[32] D.S. Jones, The scattering of sound by a simple shear layer, Phil. Trans. Roy. Soc. Lond. 284 (1323) (1977) 287–328, https://doi.org/10.1098/rsta.1977.0011.
[33] D.S. Jones, Acoustics of a splitter plate, IMA J. Appl. Math. 21 (2) (1978) 197–209, https://doi.org/10.1093/imamat/21.2.197.
[34] S.P. Koutsoyannis, Characterization of acoustic disturbances in linearly sheared flows, J. Sound Vib. 68 (2) (1980) 187–202, https://doi.org/10.1016/0022-460X(80)90464-2.
[35] S.P. Koutsoyannis, K. Karamcheti, D.C. Galant, Acoustic resonances and sound scattering by a shear layer, AIAA J. 18 (12) (1980) 1446–1454, https://doi.org/10.2514/3.7736.
[36] J.N. Scott, Propagation of sound waves through a linear shear layer, AIAA J. 17 (3) (1979) 237–244, https://doi.org/10.2514/3.61107.
[37] L.M.B.C. Campos, J.M.G.S. Oliveira, M.H. Kobayashi, On sound propagation in a linear shear flow, J. Sound Vib. 219 (5) (1999) 739–770, https://doi.org/10.1006/jsvi.1998.1880.
[38] L.M.B.C. Campos, P.G.T.A. Serrão, On the acoustics of an exponential boundary layer, Phil. Trans. Roy. Soc. Lond. 356 (1746) (1998) 2335–2378, https://doi.org/10.1098/rsta.1998.0277.
[39] L.M.B.C. Campos, M.H. Kobayashi, On the reflection and transmission of sound in a thick shear layer, J. Fluid Mech. 424 (2000) 303–326, https://doi.org/10.1017/S0022112000002068.
[40] L.M.B.C. Campos, J.M.G.S. Oliveira, On the acoustic modes in a duct containing a parabolic shear flow, J. Sound Vib. 330 (6) (2011) 1166–1195, https://doi.org/10.1016/j.jsv.2010.09.021.
[41] L.M.B.C. Campos, M.H. Kobayashi, On the propagation of sound in a high-speed non-isothermal shear flow, Int. J. Aeroacoustics 8 (3) (2009) 199–230, https://doi.org/10.1260/147547208786940035.
[42] L.M.B.C. Campos, M.H. Kobayashi, Sound transmission from a source outside a nonisothermal boundary layer, AIAA J. 48 (5) (2010) 878–892, https://doi.org/10.2514/1.40674.
[43] L.M.B.C. Campos, M.H. Kobayashi, On an acoustic oscillation energy for shear flows, Int. J. Aeroacoustics 12 (1) (2013) 123–168, https://doi.org/10.1260/1475-472X.12.1-2.123.
[44] L.M.B.C. Campos, M.H. Kobayashi, On sound emission by sources in a shear flow, Int. J. Aeroacoustics 12 (7–8) (2013) 719–742, https://doi.org/10.1260/1475-472X.12.7-8.719.
[45] M.E. Goldstein, Unsteady vortical and entropic distortions of potential flows round arbitrary obstacles, J. Fluid Mech. 89 (3) (1978) 433–468, https://doi.org/10.1017/S0022112078002682.
[46] V.V. Gobulev, H.M. Atassi, Sound propagation in an annular duct with mean potential swirling flow, J. Sound Vib. 198 (5) (1996) 601–616, https://doi.org/10.1006/jsvi.1996.0591.
[47] V.V. Gobulev, H.M. Atassi, Acoustic-vorticy waves in swirling flows, J. Sound Vib. 209 (2) (1998) 203–222, https://doi.org/10.1006/jsvi.1997.1049.
[48] L.M.B.C. Campos, P.G.T.A. Serrão, On the sound in unbounded and ducted vortex flows, SIAM J. Appl. Math. 65 (4) (2005) 1353–1368, https://doi.org/10.1137/S0036139903427076.
[49] C.K.W. Tam, L. Auriault, The wave modes in ducted swirling flows, J. Fluid Mech. 371 (1) (1998) 1–20, https://doi.org/10.1017/S0022112098002043.
[50] C.J. Heaton, N. Peake, Acoustic scattering in a duct with mean swirling flow, J. Fluid Mech. 540 (2005) 189–220, https://doi.org/10.1017/S0022112005005719.
[51] C.J. Heaton, N. Peake, Algebraic and exponential instability of inviscid swirling flow, J. Fluid Mech. 565 (2006) 279–318, https://doi.org/10.1017/S0022112006001698.
[52] L.M.B.C. Campos, P.G.T.A. Serrão, On the continuous and discrete spectrum of acoustic-vortical waves, Int. J. Aeroacoustics 12 (7–8) (2013) 743–782, https://doi.org/10.1260/1475-472X.12.7-8.743.
[53] H. Posson, N. Peake, The acoustic analogy in an annular duct with swirling mean flow, J. Fluid Mech. 726 (2013) 439–475, https://doi.org/10.1017/jfm.2013.210.
[54] L.M.B.C. Campos, On the generalization to swirling flows of Lighthill's eighth-power law. Part I: waves in axisymmetric sheared and swirling isentropic flows, Int. J. Aeroacoustics 15 (3) (2016) 276–293, https://doi.org/10.1177/1475472X16630850.
[55] L.M.B.C. Campos, On the generalization to swirling flows of Lighthill's eighth-power law. Part II: laws of intensity of radiation for acoustic-vortical waves, Int. J. Aeroacoustics 15 (8) (2016) 690–711, https://doi.org/10.1177/1475472X16666631.
[56] J.R. Mathews, N. Peake, The acoustic Green's function for swirling flow in a lined duct, J. Sound Vib. 395 (2017) 294–316, https://doi.org/10.1016/j.jsv.2017.02.015.
[57] J.R. Mathews, N. Peake, The acoustic Green's function for swirling flow with variable entropy in a lined duct, J. Sound Vib. 419 (2017) 630–653, https://doi.org/10.1016/j.jsv.2017.08.010.
[58] C. Carathéodory, Theory of Functions of a Complex Variable, vols. 1–2, Verlag Birkhauser, 1950. ISBN:9780821828311.
[59] A. Erdélyi (Ed.), Higher Transcendental Functions, vols. 1–3, McGraw-Hill, 1953, ASIN: B005Z5A43I.
[60] Z.X. Wang, D.R. Guo, Special Functions, World Scientific, 1989. ISBN:9789971506599.
[61] A. Gray, G.B. Mathews, A Treatise on Bessel Functions and Their Applications to Physics, Macmillan, 1895 (reprint).
[62] N.W. MacLachlan, Bessel Functions for Engineers, Oxford University, 1934.
[63] G.N. Watson, A Treatise on the Theory of Bessel Functions, Cambridge University, 1944.
[64] A.R. Forsyth, A Treatise on Differential Equations, Dover, 1929. ISBN:9780486693149.
[65] E.G.C. Poole, Introduction to the Theory of Linear Differential Equations, Clarendon Press, 1936.
[66] E.L. Ince, Ordinary Differential Equations, Dover, 1956. ISBN:9780486603490.
[67] A. Michalke, On spatially growing disturbances in an inviscid shear layer, J. Fluid Mech. 23 (3) (1965) 521–544, https://doi.org/10.1017/S0022112065001520.
[68] A. Michalke, Instability of a Compressible Circular Free Jet with Consideration of the Influence of the Jet Boundary Layer Thickness, Technical Memorandum TM 75190, NASA, 1977.
[69] S.E.P. Bergliaffa, K. Hibberd, M. Stone, M. Visser, Wave equation for sound in fluids with vorticity, Physica D 191 (1–2) (2004) 121–136, https://doi.org/10.1016/j.physd.2003.11.007.
[70] E. Kamke, Differentialgleichungen Lösungsmethoden und Lösungen, vol. 1, Chelsea Publishing Company, New York, 1971. ISBN:9783519120179.
[71] A. Ronveaux (Ed.), Heun's Differential Equations, Oxford University Press, Oxford, England, 1995, ISBN:9780198596950.
[72] M. Abramowitz, I.A. Stegun (Eds.), Handbook of Mathematical Functions, Vol. 55 of Dover Books on Advanced Mathematics, Dover, 1965, ISBN:9780486612720.
[73] T. Bromwich, T.M. MacRobert, An Introduction to the Theory of Infinite Series, MacMillan, 1926. ISBN:9781164810001.
[74] K. Knopp, Theory and Application of Infinite Series, reprint, Dover, 1990, p. 1921. ISBN:9780486661650.
[75] E.T. Whittaker, G.N. Watson, A Course of Modern Analysis, Cambridge UP, 1927. ISBN:9781603864541.
[76] L.M.B.C. Campos, Transcendental Representations with Applications to Solids and Fluids, Vol. 2 of Mathematics and Physics in Science and Engineering, CRC Press, 2012. ISBN:9781439834312.
[77] L.M.B.C. Campos, J.F.P.G. Leitão, On the computation of special functions with applications to non-linear and inhomogeneous waves, Comput. Mech. 3 (5) (1988) 343–360, https://doi.org/10.1007/BF00712148.
[78] C.C. Lin, The Theory of Hydrodynamic Stability, Cambridge Monographs on Mechanics Applied Mathematics, Cambridge U.P., 1955. aSIN: B0000CJB1L.

[79] S. Chandrasekhar, Hydrodynamic and Hydromagnetic Stability, Oxford U.P., 1961. ISBN:978–0486640716.
[80] D.D. Joseph, Stability of Fluid Motions. I,II, Vol. 27 & 28 of Encyclopedia of Physics, Springer-Verlag, 1976. ISBN:9780471116219.
[81] P.G. Drazin, W.H. Reid, Hydrodynamic Stability, Cambridge Monographs on Mechanics and Applied Mathematics, Cambridge U.P., 1981. ISBN:0521227984.
[82] J. Pedlosky, Geophysical Fluid Dynamics, Springer, 1979. ISBN:9781468400717.
[83] L.M.B.C. Campos, On three-dimensional acoustic-gravity waves in model non-isothermal atmospheres, Wave Motion 5 (1) (1983) 1–14, https://doi.org/10.1016/0165-2125(83)90002-1.
[84] L.M.B.C. Campos, On waves in gases. part II: interacion of sound with magnetic and internal modes, Rev. Mod. Phys. 59 (2) (1987) 363–462, https://doi.org/10.1103/RevModPhys.59.363.